

Tau Signals at the Tevatron for Gauge Mediated Supersymmetry Breaking

D. J. Muller and S. Nandi

*Department of Physics, Oklahoma State University,
Stillwater, Oklahoma 74078*

(November 1998)

Abstract

We consider the phenomenology of GMSB models where the lighter stau is the next to lightest supersymmetric particle. In this situation, the dominant signals for supersymmetry are events with two or three high p_T τ leptons accompanied by large missing transverse energy. We find that the inclusive two τ -jets signature could be observable at the Tevatron's Run II, while the inclusive three τ -jets signature could be important at Run III.

arXiv:hep-ph/9811248v1 4 Nov 1998

I. INTRODUCTION

The phenomenology of gauge mediated supersymmetry breaking (GMSB) models have been the subject of much interest lately [1–3]. They provide an alternative to the usually considered case of the soft terms involving the low energy fields induced by gravity. In GMSB models the supersymmetry (SUSY) breaking is communicated to the visible sector by gauge fields. The scale at which this occurs is usually taken to be around 10^5 GeV.

The sparticle spectrum in GMSB models has some significant differences from the usual gravity mediated SUSY breaking models. In GMSB models, the gravitino is the lightest supersymmetric particle (LSP). The next to lightest supersymmetric particle (NLSP) is typically the lightest neutralino or the lighter stau. Most phenomenological studies and experimental searches that have been performed in the context of GMSB have taken the lightest neutralino to be the NLSP. The lightest neutralino then decays by $\chi_1^0 \rightarrow \gamma \tilde{G}$. If this decay takes place within the detector, the signal involves high p_T photons accompanied by large \cancel{E}_T [4]. For much of the parameter space, however, the lighter of the two scalar staus is the NLSP. In this case, the decays of SUSY particles produce the $\tilde{\tau}_1$ which subsequently decays to a τ and the gravitino. If the $\tilde{\tau}_1$ decays occur within the detector, signatures for SUSY production will then generally include τ leptons from the $\tilde{\tau}_1$ decays and \cancel{E}_T due to the stable gravitinos and neutrinos leaving the detector.

It was proposed that GMSB models where the $\tilde{\tau}_1$ is the NLSP can lead to unusual and distinguishing signatures for SUSY production at colliders [5]. At the Tevatron, these signals arise from chargino pair production ($\chi_1^+ \chi_1^-$) and from the production of the chargino with the next to lightest neutralino ($\chi_1^\pm \chi_2^0$). Slepton pair production ($\tilde{l}_1^+ \tilde{l}_1^-$ where $l = e, \mu, \text{ or } \tau$) can also be significant. The subsequent decays typically involve high p_T τ leptons and substantial \cancel{E}_T . In this paper we analyze the signals for such SUSY production at the Tevatron. In particular we consider the parameters for the $n = 2$ stau NLSP model line of the Gauge Mediation/Low Scale SUSY Breaking working group of the Physics at Run II Supersymmetry/Higgs workshop.

II. MASS SPECTRUM AND PRODUCTION MECHANISMS

Since the observed signal depends on the masses of the sparticles, we first begin by describing the model and the corresponding mass spectrum. In our model, the messenger sector consists of some number of multiplets that are $\bar{5} + 5$ representations of SU(5). They couple to a chiral superfield S in the hidden sector whose scalar component has a vacuum expectation value (VEV) $\langle s \rangle$ and whose auxiliary component has a VEV $\langle F_s \rangle$. By imposing the requirement that the electroweak (EW) symmetry is broken radiatively, the particle spectrum and the mixing angles depend on five parameters: M , Λ , n , $\tan \beta$ and the sign of μ . M is the messenger scale. Λ is equal to $\langle F_s \rangle / \langle s \rangle$ and is related to the SUSY breaking scale. The parameter n is dictated by the choice of the vector-like messenger sector and can take the values 1, 2, 3, or 4 to satisfy the perturbative unification constraint. The definition of $\tan \beta$ is taken as $\tan \beta \equiv v_2 / v_1$ where v_2 is the VEV for the up-type (H_u) Higgs doublet and v_1 is the VEV for the down-type (H_d) Higgs doublet. The parameter μ is the coefficient in the bilinear term, $\mu H_u H_d$, in the superpotential. Constraints coming from $b \rightarrow s \gamma$ strongly favor negative values for μ in our convention [6] and, in the cases considered in this work,

μ is taken to be negative. Demanding that the EW symmetry be broken radiatively fixes the magnitude of μ and the parameter B (from the $B\mu H_u H_d$ term in the scalar potential) in terms of the other parameters of the theory.

The soft SUSY breaking gaugino and scalar masses at the messenger scale are given by [1,7]

$$\tilde{M}_i(M) = n g\left(\frac{\Lambda}{M}\right) \frac{\alpha_i(M)}{4\pi} \Lambda \quad (1)$$

and

$$\tilde{m}^2(M) = 2n f\left(\frac{\Lambda}{M}\right) \sum_{i=1}^3 k_i C_i \left(\frac{\alpha_i(M)}{4\pi}\right)^2 \Lambda^2 \quad (2)$$

where the α_i are the three SM gauge couplings and $k_i = 1, 1$ and $3/5$ for SU(3), SU(2), and U(1), respectively. The C_i are zero for gauge singlets and are $4/3, 3/4$ and $(Y/2)^2$ for the fundamental representations of SU(3), SU(2) and U(1), respectively (with Y given by $Q = I_3 + Y/2$). $g(x)$ and $f(x)$ are messenger scale threshold functions. We calculate the sparticle masses at the scale M using Eqs. (1) and (2) and run these to the electroweak scale using the appropriate renormalization group equations [8].

The decay chains and hence the signatures for the events depend on the particles initially produced as well as the hierarchy of the masses. Since SUSY breaking is communicated to the visible sector by gauge interactions, the mass differences between the superparticles depend on their gauge interactions. This creates a hierarchy in mass between electroweak and strongly interacting sparticles. Eq. (1) shows that the gluino is more massive than the EW charginos and neutralinos, while Eq. (2) shows that squarks are considerably more massive than sleptons. Given this hierarchy of sparticle masses and the current lower bounds on squark and gluino masses, the production of strongly interacting sparticles is probably not a viable search mode for SUSY at the Tevatron Run II. A more likely mechanism for producing SUSY particles is via EW gaugino production. At the Tevatron, chargino pair ($\chi_1^+ \chi_1^-$) production takes place through s-channel Z and γ exchange and $\chi_2^0 \chi_1^\pm$ production is through s-channel W exchange. Squark exchange via the t-channel also contributes to both processes, but the contributions are expected to be negligible since the squark masses are large in GMSB models. The production of $\chi_1^0 \chi_1^\pm$ is suppressed due to the smallness of the coupling involved. In regions of the parameter space where the production of charginos and neutralinos is kinematically suppressed, the pair production of sleptons ($\tilde{\tau}_1 \tilde{\tau}_1, \tilde{\mu}_1 \tilde{\mu}_1$ and $\tilde{e}_1 \tilde{e}_1$) can be important. Their production occurs through s-channel Z and γ exchange.

Given the hierarchy of sparticle masses in GMSB models, there are roughly four possible cases to consider for SUSY production at the Tevatron:

Case 1: $m_{\tilde{\nu}} > M_{\chi_2^0} \gtrsim M_{\chi_1^\pm} > m_{\tilde{e}_1, \tilde{\mu}_1} > M_{\chi_1^0} > m_{\tilde{\tau}_1}$

Case 2: $M_{\chi_2^0} \gtrsim M_{\chi_1^\pm} > m_{\tilde{\nu}} > M_{\chi_1^0} > m_{\tilde{e}_1, \tilde{\mu}_1} > m_{\tilde{\tau}_1}$

Case 3: $M_{\chi_2^0} \gtrsim M_{\chi_1^\pm} > m_{\tilde{\nu}} > m_{\tilde{e}_1, \tilde{\mu}_1} > M_{\chi_1^0} > m_{\tilde{\tau}_1}$

Case 4: $m_{\tilde{\nu}} > M_{\chi_2^0} \gtrsim M_{\chi_1^\pm} > M_{\chi_1^0} > m_{\tilde{e}_1, \tilde{\mu}_1} > m_{\tilde{\tau}_1}$

The three sneutrino masses are nearly the same. The lighter of the selectrons and smuons are essentially right handed and have the same mass. Also, for all the parameter points we considered, χ_1^\pm and χ_2^0 are nearly degenerate in mass.

The possible final state configurations at the Tevatron depend on the sparticle spectrum, but they will have certain aspects in common. Since the $\tilde{\tau}_1$ is the NLSP, the various possible decay modes will (usually) produce at least two τ leptons arising from the decays of the $\tilde{\tau}_1$'s. In addition, there can also be large \cancel{E}_T due to the stable gravitinos and neutrinos escaping detection.

A special situation in cases 2 and 4 arises when the lighter selectron and the lighter smuon are nearly degenerate in mass to the lighter stau. When the mass difference between the selectron and the stau is less than twice the mass of the τ , essentially the only decay mode for the selectron is $\tilde{e} \rightarrow e\tilde{G}$. The lighter smuon likewise decays via $\tilde{\mu} \rightarrow \mu\tilde{G}$. This situation is referred to as the ‘‘co-NLSP’’ case [9].

III. ANALYSIS AND RESULTS

We now give a detailed analysis of the possible Tevatron signatures for SUSY production in the context of GMSB models where the lighter stau is the NLSP and decays promptly within the detector. This analysis is performed in the context of the Main Injector (MI) and TeV33 upgrades of the Tevatron collider. The center of mass energy is taken to be $\sqrt{s} = 2\text{ TeV}$ and the integrated luminosity is taken to be 2 fb^{-1} for the MI upgrade and 30 fb^{-1} for the TeV33 upgrade [10].

In performing this analysis, the cuts employed are that final state charged leptons must have $p_T > 10\text{ GeV}$ and a pseudorapidity, $\eta \equiv -\ln(\tan\frac{\theta}{2})$ where θ is the polar angle with respect to the proton beam direction, of magnitude less than 1. Jets must have $E_T > 10\text{ GeV}$ and $|\eta| < 2$. In addition, hadronic final states within a cone size of $\Delta R \equiv \sqrt{(\Delta\phi)^2 + (\Delta\eta)^2} = 0.4$ are merged to a single jet. Leptons within this cone radius of a jet are discounted. For a τ -jet to be counted as such, it must have $|\eta| < 1$. The most energetic τ jet is required to have $E_T > 20\text{ GeV}$. In addition, a missing transverse energy cut of $\cancel{E}_T > 30\text{ GeV}$ is imposed.

We consider each mass case in turn. In our analysis, we restrict ourselves to those regions of the parameter space where the $\tilde{\tau}_1$ decays promptly to a τ and a gravitino. The parameter space is also restricted to those regions where $m_{\tilde{\tau}_1} \gtrsim 70\text{ GeV}$. Results from LEP-2 set a lower bound of $m_{\tilde{\tau}_1} \geq 72\text{ GeV}$ [12].

IV. STAU NLSP LINE WITH $N = 2$

In this section we do the analysis for points along the line defined by the parameter values $M/\Lambda = 3$, $n = 2$ and $\tan\beta = 15$. We vary Λ from 35 TeV to 85 TeV. The masses for the sparticles that are of interest here are given in Fig. 1. Note that the sneutrino mass is always above that of the lightest chargino and the lightest two neutralinos. Thus the sneutrinos do not figure into the decay chains of the major SUSY production mechanisms here. Note that the lightest neutralino is below the selectron/smuon mass at the lower end of the Λ scale ($\Lambda \lesssim 45\text{ TeV}$). Thus for $\Lambda \lesssim 45\text{ TeV}$ the mass spectrum is of type 1. For $\Lambda \gtrsim 45\text{ TeV}$, the mass spectrum is of type 4. In this region of Λ , there are more decay modes

for the various particles due to the increasing masses of all the sparticles as well as the shift in the position of the lightest neutralino in the mass hierarchy.

The cross sections for these parameters are given in Fig. 2. From the figure, the cross sections for $\chi_1^+\chi_1^-$ and $\chi_2^0\chi_1^\pm$ production dominate for the region where Λ is below 65 TeV. As Λ increases, the masses of the gauginos increase significantly and hence the cross section falls off. For $\Lambda \gtrsim 70$ TeV, the production rates for $\tilde{\tau}_1^+\tilde{\tau}_1^-$ and $\tilde{e}_1^+\tilde{e}_1^-$ are dominant, but the cross sections tend to be rather low.

The signature depends on the allowed decay modes of the sparticles and their branching ratios. The branching ratios for the sparticles of interest are given in Table I. Since $\tilde{\tau}_1$ is the NLSP, it decays via $\tilde{\tau}_1 \rightarrow \tau \tilde{G}$. The decays of the selectron and smuon depend strongly on the value of Λ . For Λ below ~ 45 TeV, the lightest neutralino has a mass below that of $\tilde{\mu}_1$ and \tilde{e}_1 . As a consequence of this, the main decay mode of lightest smuon is $\tilde{\mu}_1 \rightarrow \chi_1^0 \mu$ and the main decay mode of the lightest selectron is $\tilde{e}_1 \rightarrow \chi_1^0 e$. For higher values of Λ , however, the lightest neutralino mass increases above that of \tilde{e}_1 and $\tilde{\mu}_1$. Then the only available two-body decay mode for the lightest smuon is $\tilde{\mu}_1 \rightarrow \mu \tilde{G}$ with the corresponding decay mode for the lightest selectron. Given the smallness of the coupling involved, though, the possibility exists that some three-body decays could be important. Indeed, the neutralino mediated decays $\tilde{\mu}_1^- \rightarrow e^- \tau^- \tilde{\tau}^+$ and $\tilde{\mu}_1^- \rightarrow e^- \tau^+ \tilde{\tau}^-$ are the important decay modes [11] for these higher values of Λ .

Since the lightest neutralino tends to be one of the least massive sparticles, its only decay modes are $\chi_1^0 \rightarrow \tilde{\tau}_1 \tau$ and the decays to $\tilde{\mu}_1$ and \tilde{e}_1 if χ_1^0 is greater in mass than those sparticles. Since the lightest neutralino is less massive than the selectrons and smuons for Λ , the only decay mode is $\chi_1^0 \rightarrow \tilde{\tau}_1 \tau$. As Λ increases above 45 TeV, $\tilde{\mu}_1$ and \tilde{e}_1 become increasingly important, although $\chi_1^0 \rightarrow \tilde{\tau}_1 \tau$ remains the dominant decay mode.

Since the lightest chargino is mostly wino, it couples mainly to “left-handed” sfermions. Thus the decay mode $\chi_1^\pm \rightarrow \tilde{\tau}_1 \nu_\tau$ is typically important due to the significant mixing of the left-handed and right-handed staus and the lower mass of the $\tilde{\tau}_1$. This decay mode is, in fact, essentially the only decay mode for low values of Λ with the parameters considered here. Thus with the subsequent decay $\tilde{\tau}_1 \rightarrow \tau \tilde{G}$, there are typically two τ leptons produced in $\chi_1^+\chi_1^-$ production at these values of Λ . As Λ increases, however, the decay mode $\chi_1^\pm \rightarrow \chi_1^0 W$ becomes available and becomes the dominant decay mode as Λ increases above 60 TeV. With the two τ leptons that can be expected from the lightest neutralino decay and the $W \rightarrow \tau \nu_\tau$ decay, we can expect up to six τ leptons from $\chi_1^+\chi_1^-$ production at these larger values of Λ .

There are many decay modes for the second lightest neutralino as Table I shows. For low values of Λ , the dominant decay mode is $\chi_2^0 \rightarrow \tilde{\tau}_1 \tau$ at 50 - 60%. The decays to the other sleptons are also important at 15 - 20%. Thus $\chi_1^\pm \chi_2^0$ production produces three τ leptons: two from the slepton decays of the neutralino and one from the decay $\chi_1^\pm \rightarrow \tilde{\tau}_1 \nu_\tau$ followed by $\tilde{\tau}_1 \rightarrow \tau \tilde{G}$. As Λ increases above 55 TeV, The decay $\chi_2^0 \rightarrow \chi_1^0 h$, where h is the Higgs boson, rapidly becomes the dominant decay mode. The decay $\chi_2^0 \rightarrow \chi_1^0 Z$ is also present, but of relatively little importance.

Given the cuts that we place on the τ -jets, the question arises as to how high we can expect the E_T of the τ -jets to be. Fig. 3 gives the E_T distribution of the highest E_T τ -jet for $\Lambda = 35$ TeV. The pseudorapidity cut of $|\eta| < 1$ on τ -jets has been imposed in Fig. 3(b). The peak in the distribution occurs at about 25 GeV with a broad tail that reaches out beyond 120 GeV. Thus the leading τ -jets are relatively hard and many will pass the transverse

energy cut of $E_T > 20$ GeV. The next to highest E_T τ -jet is significantly different as Fig. 4 shows. Here the distribution peaks at a lower value of about 15 GeV and hardly extends at all beyond 80 GeV. Due to the softness of the secondary τ -jets, many of the τ -jets will tend to be eliminated by the cuts.

Also of interest is the \cancel{E}_T distribution. With energetic and stable gravitinos and neutrinos produced in the decays, it is expected that large missing transverse energy could be an important part of the signal. Since the missing transverse energy is calculated from what is observed, however, the question arises as to whether significant cancellation occurs due to the many decay products. Fig. 5 gives the \cancel{E}_T distribution for the case where $\Lambda = 35$ TeV. The figure demonstrates that the \cancel{E}_T distribution is indeed broad with a tail reaching out beyond 120 GeV. The peak before cuts occurs at about 35 GeV and the peak still occurs at about 35 GeV when E_T/p_T and pseudorapidity cuts are applied to the various particles. Thus a 30 GeV cut should not be too restrictive. As Λ is increased, the \cancel{E}_T distribution gets harder since the gaugino masses get larger as Λ is increased.

We now consider the specifics of the various final state possibilities. Table II give the inclusive branching ratios for different number of τ -jets for $\Lambda = 35$ TeV. As indicated above, this example always produces two τ leptons in chargino pair production. Before cuts the inclusive branching ratio for the 2 τ -jet mode in chargino pair production is 42%, while the 1 τ -jet mode in chargino pair production is 45.6%. After the cuts specified above, the branching ratios are cut down rather substantially. The one τ -jet BR becomes 25.8% and the two τ -jet BR is 10.8%. The situation changes as Λ increases. This is demonstrated in Tables III and IV which are for $\Lambda = 50$ and 70 TeV, respectively. We see that there is now the possibility for many more τ -jets. This is due to the appearance of the decay mode $\chi_1^\pm \rightarrow \chi_1^0 W$. With the decay $\chi_1^0 \rightarrow \tilde{\tau}_1 \tau$ followed by $\tilde{\tau}_1 \rightarrow \tau \tilde{G}$ along with the decay $W \rightarrow \tau \nu_\tau$, there is now the possibility for producing up to six τ -jets. At $\Lambda = 50$ TeV, the BR for three τ -jets is 16.3%. This is cut down substantially after cuts, however, and the BR becomes only 1%. $\Lambda = 70$ TeV shows similar results, although at this point this point the cross section for $\chi_1^+ \chi_1^-$ production is low.

Considering $\chi_2^0 \chi_1^\pm$ production, we recall that at $\Lambda \lesssim 45$ TeV, the decay modes of χ_2^0 are $\chi_2^0 \rightarrow \tilde{\tau}_1 \tau$, $\chi_2^0 \rightarrow \tilde{\mu}_1 \mu$ and $\chi_2^0 \rightarrow \tilde{e}_1 e$. With the subsequent decays $\tilde{\tau}_1 \rightarrow \tau \tilde{G}$ and $\tilde{\mu}_1 \rightarrow \mu \tau \tilde{\tau}_1$ along with the corresponding decay of the selectron, the number of τ leptons from χ_2^0 decay is two. With the one τ lepton from the chargino, we have up to three τ leptons from $\chi_2^0 \chi_1^\pm$ production at these values of Λ . We see from Table II that for $\Lambda = 35$ TeV, the branching ratios for inclusive production of 3 τ -jets is 27.2% before cuts, while for 1 and 2 τ -jets the branching ratios are 24% and 44.3%, respectively. These branching ratios are cut back considerably once the cuts are included. The 3 τ -jet BR in particular is reduced to only 2.6%. As Λ increases, the potential exists to create more than three τ -jets due to the new decay modes for χ_1^\pm and χ_2^0 . The branching ratios for more than three τ -jets tend to be small after cuts, however, as Tables III and IV demonstrate.

Slepton production tends to be rather simple since there are relatively few decay modes available to the sleptons. This is especially true for the production of the lighter stau as its only significant decay mode is $\tilde{\tau}_1 \rightarrow \tau \tilde{G}$. Thus for $\tilde{\tau}_1^+ \tilde{\tau}_1^-$ production up to two τ -jets are possible. Before cuts, the 2 τ -jet BR is 42% and the 1 τ -jet BR is 45.6% for $\tilde{\tau}_1^+ \tilde{\tau}_1^-$ production independent of the values of Λ considered. After cuts, these drop down to 10 - 17% and 30 - 40%, respectively, as shown in Tables II, III and IV. The three-body decay modes of the

lightest selectron and smuon mean that up to four τ -jets are possible in $\tilde{\mu}_1^+ \tilde{\mu}_1^-$ production and $\tilde{e}_1^+ \tilde{e}_1^-$ production. The branching ratios for three and four τ -jets in $\tilde{e}_1^+ \tilde{e}_1^-$ and $\tilde{\mu}_1^+ \tilde{\mu}_1^-$ production are greatly diminished after cuts.

The question now arises as to the observability of these modes at the Tevatron's Run II. The cross sections for inclusive τ -jet production before cuts are given in Fig. 6. All the SUSY production modes considered in this analysis are included. Events with more than four τ -jets are not included in the figure due to their extremely low branching ratios. By far the dominant decay mode is the 2 τ -jets mode. The 3 τ -jets and 1 τ -jet modes are also quite large.

Of course, the real issue is what the production cross sections are after the cuts have been imposed. These are given in Fig. 7. The graph shows that after cuts, the 1 τ -jet mode is dominant. The 2 τ -jets mode is of the same order of magnitude and the 3 τ -jet mode is not unappreciable. For $\Lambda = 35$ TeV, the three τ -jets rate is 4.7 fb. For an integrated luminosity of 2 fb^{-1} (approximately what is expected initially during Run II), this corresponds to ~ 9 observable events. For 30 fb^{-1} , the number of observable events is 141. The 2 τ -jets cross sections of 48.1 fb gives ~ 96 events for 2 fb^{-1} of data and ~ 1440 for 30 fb^{-1} of data. As Λ increases, the numbers are smaller due to the smaller SUSY production rate. For $\Lambda = 50$ TeV, the expected number of events for three τ -jets is about 2 for 2 fb^{-1} of data and 30 for 30 fb^{-1} of data. The expected number of 2 τ -jets events is 16 and 248 for 2 fb^{-1} and 30 fb^{-1} of data, respectively. For $\Lambda = 70$ TeV, the expected number of events for two τ -jets is 2 and 28 for 2 fb^{-1} and 30 fb^{-1} , respectively.

The branching ratios for some of the more interesting individual modes in combined SUSY production are given in Table V. The electrons and muons are typically the soft to pass the cuts. Thus requiring an e or μ to enhance the signal over background probably will be of little help.

V. STAU NLSP LINE WITH $N = 3$

We now consider a case where the ordering of the sparticles masses is quite different from the previous case. The parameters taken here are $n = 3$, $\tan \beta = 15$ and $M/\Lambda = 20$. We vary Λ from 25 to 55 TeV. The masses for these parameters are given in Fig. 8. We see that the ordering of the masses is of type 2: $M_{\chi_2^0} \gtrsim M_{\chi_1^\pm} > m_{\tilde{\nu}} > M_{\chi_1^0} > m_{\tilde{e}_1, \tilde{\mu}_1} > M_{\tilde{\tau}_1}$. This case is more complicated than the previous one due to the shifting of the sneutrino masses below that of χ_1^\pm and χ_2^0 . As a consequence, there are many decay modes for χ_1^\pm and χ_2^0 over the parameter space considered here. Moreover, the lightest selectron and smuon masses are always below that of the lightest neutralino. The result of all this is that the decay chains will generally be quite involved with many steps for the values of Λ considered here.

The branching ratios for the sparticles are given in Table VI. Since the masses of the lightest selectron and the lightest smuon are always below that of the lightest neutralino, there are three decay modes available for the values of Λ considered: $\chi_1^0 \rightarrow \tilde{\tau}_1 \tau$, $\chi_1^0 \rightarrow \tilde{\mu}_1 \mu$ and $\chi_1^0 \rightarrow \tilde{e}_1 e$. The decay to the stau is the dominant decay mode especially at low values of Λ .

There are many potential decay modes for the chargino with these values of the parameters. Since the sneutrinos are now less massive than the chargino, these provide three decay modes that were not present in the previous case: $\chi_1^\pm \rightarrow \tilde{\nu}_\tau \tau$, $\chi_1^\pm \rightarrow \tilde{\nu}_\mu \mu$ and $\chi_1^\pm \rightarrow \tilde{\nu}_e e$.

For the entire range of parameters considered, these decays to the sneutrinos are always present as well as the decay $\chi_1^\pm \rightarrow \tilde{\tau}_1 \nu_\tau$ which is the dominant decay mode for Λ less than about 50 TeV. As Λ increases, the mass difference between the lightest chargino and the lightest neutralino increases and the decay $\chi_1^\pm \rightarrow \chi_1^0 W$ becomes kinematically allowed. At $\Lambda = 55$ TeV, it is as important a decay mode as $\chi_1^\pm \rightarrow \tilde{\tau}_1 \nu_\tau$. One other distinguishing characteristic of this case from the last one is that the heavier selectron and smuon have masses below that of χ_1^\pm and χ_2^0 . Thus the decays $\chi_1^\pm \rightarrow \tilde{\tau}_2 \nu_\tau$, $\chi_1^\pm \rightarrow \tilde{\mu}_2 \nu_\mu$ and $\chi_1^\pm \rightarrow \tilde{e}_2 \nu_e$ are available and their branching ratios are small, but not unimportant at large Λ .

For the second lightest neutralino, there are up to eleven main decay modes. For low values of Λ the dominant decay mode is $\chi_2^0 \rightarrow \tilde{\tau}_1 \tau$. The other slepton decay modes $\chi_2^0 \rightarrow \tilde{e}_1 e$ and $\chi_2^0 \rightarrow \tilde{\mu}_1 \mu$ are also important. As Λ increases, the decay $\chi_2^0 \rightarrow \chi_1^0 h$ becomes kinematically allowed and rapidly becomes the dominant decay. The decay modes to the sneutrinos also become more important.

The E_T distribution of the leading τ -jet for $\Lambda = 25$ TeV is given in Fig. 10 and the E_T distribution of the secondary τ -jet is given in Fig. 11. The distribution for the leading τ -jet is quite similar to the previous case, but the secondary τ -jet spectrum is softer due to the decrease in the direct production of τ leptons from chargino and neutralino decays and more of the τ leptons coming from further down the decay chain. The \cancel{E}_T distribution is given in Fig. 12.

We now consider the details of the various final state possibilities. Table VII gives the inclusive branching ratios for different numbers of τ -jets for $\Lambda = 25$ TeV. In principle, up to six τ leptons can be produced in $\chi_1^+ \chi_1^-$ production, but the five and six τ lepton branching ratios are small. The most important mode before cuts is the two τ -jet mode at 40.4%, but the one and three τ -jets modes are also appreciable. After implementing the cuts, the branching ratios are greatly decreased: the two τ -jets branching ratio becomes only 11.4% and the one τ -jet branching ratio becomes 23.4%. The three τ -jet branching ratio becomes essentially negligible. The situation changes as Λ increases. Table VIII gives the inclusive τ -jet branching ratios for $\Lambda = 40$ TeV. The branching ratio for greater numbers of τ -jets are now larger. This is due to the decrease in the branching ratio for $\chi_1^\pm \rightarrow \tilde{\tau}_1 \nu_\tau$ from which one can get only one τ -jet from the chargino and the increase in $\chi_1^\pm \rightarrow \chi_1^0 W$ which can give three τ -jets and $\chi_1^\pm \rightarrow \tilde{\nu}_\tau \tau$ which can also give three τ -jets. The two τ -jets mode in $\chi_1^+ \chi_1^-$ production is still dominant at 34.8%, but now the three τ -jets mode is appreciable at 28.6%. After cuts, the three τ -jets rate drops to 5% and the one τ -jet mode becomes dominant at 30.1%.

Turning now to $\chi_2^0 \chi_1^\pm$ production, we see that at low Λ , there is the potential to produce up to five τ -jets (three from $\chi_1^\pm \rightarrow \tilde{\nu}_\tau \tau$ with the subsequent decays $\tilde{\nu}_\tau \rightarrow \chi_1^0 \nu_\tau$ and $\chi_1^0 \rightarrow \tilde{\tau}_1 \tau$ and two τ -jets from $\chi_2^0 \rightarrow \tilde{\nu}_\tau \nu_\tau$), but the branching ratios for more than three τ -jets are rather small. As usual the dominant decay mode is to two τ -jets with a before cuts branching ratio of 40.8%, but the three τ -jets branching ratio is large at 29.1% as shown in Table VII. After cuts these fall to 16.8% and 3.3%, respectively. The one τ -jet mode becomes dominant with a branching ratio of 24.5%. Table VIII gives the results for $\Lambda = 40$ TeV. The four τ -jets mode has a substantial decay rate before cuts, but this mode becomes negligible after cuts due to the softness of the fourth τ -jet due to its production further down the decay chain. On the other hand, the three τ -jets branching ratio is now higher at 6.7%.

Slepton production for this case is largely the same as in the previous case. With $\tilde{\tau}_1 \rightarrow \tau \tilde{G}$

being essentially the only decay mode for the lighter stau, the τ -jet branching ratios before cuts are completely dictated by the hadronic branching ratio for the τ lepton. For $\tilde{\mu}_1^+ \tilde{\mu}_1^-$ and $\tilde{e}_1^+ \tilde{e}_1^-$ production, up to four τ -jets can be produced, but after cuts the rates for three and four τ -jets are greatly reduced.

Putting all the pieces together, we can now answer the question as to the probability of observing these events at Tevatron's Run II and Run III. Fig. 13 shows the branching ratios for the inclusive τ -jet modes before cuts for all the considered SUSY production modes combined. The two τ -jets mode is the mode with the largest $\sigma \cdot \text{BR}$, but the production rates for one and three τ -jets are close to this. After including cuts, the one τ -jet mode is dominant and the two τ -jets mode is respectably high as seen in Fig. 14. For $\Lambda = 25 \text{ TeV}$, the three τ -jet rate is 5.4 fb giving ~ 11 for 2 fb^{-1} of data and ~ 162 events for 30 fb^{-1} of data. The two τ -jet rate of 39.3 fb gives ~ 79 and ~ 1179 events, respectively. For the higher Λ value of 50 TeV , the rates are cut down significantly. The two τ -jets rate of 1.0 fb gives ~ 2 and ~ 30 events for 2 fb^{-1} and 30 fb^{-1} of data, respectively.

VI. CO-NLSP CASE

The co-NLSP case [9] refers to when the mass difference between \tilde{e}_1 (and $\tilde{\mu}_1$) and $\tilde{\tau}_1$ is less than the mass of the τ lepton. When this is the case, the three-body decay mode $\tilde{e}_1 \rightarrow e\tau\tilde{\tau}_1$ is not kinematically allowed and the main decay mode for the selectron is the two-body mode $\tilde{e}_1 \rightarrow e\tilde{G}$. The parameters for the example of this case that is considered here are $n = 3$, $\tan\beta = 3$ and $M/\Lambda = 3$. Λ is varied from 25 to 65 TeV. The masses of the sparticles of interest are given in Fig. 15. We see that the ordering of the masses here is a special case of type 2: $M_{\chi_2^0} \gtrsim M_{\chi_1^\pm} > m_{\tilde{\nu}} > M_{\chi_1^0} > m_{\tilde{e}_1, \tilde{\mu}_1} \approx m_{\tilde{\tau}_1}$. With this ordering of the masses there are typically many decay modes of the sparticles to consider. The cross sections for the SUSY production modes are given in Fig. 16. Due to the rapid increase in the sparticle masses (especially the gaugino masses) as Λ is increased, the cross sections tend to decrease fairly rapidly.

The branching ratios for the sparticles of interest are given in Table XI. Since the lighter selectron and the lighter smuon have about the same mass as the stau, the branching ratios for $\chi_1^0 \rightarrow \tilde{\tau}_1\tau$, $\chi_1^0 \rightarrow \tilde{\mu}_1\mu$ and $\chi_1^0 \rightarrow \tilde{e}_1e$ are nearly equal. The decay to the stau is slightly favored.

The chargino's decays strongly depend on the value of Λ . For values of Λ that are 30 TeV and below, the dominant decay mode of the chargino is $\chi_1^\pm \rightarrow \tilde{\tau}_1\nu_\tau$. As Λ is increased above this, the chief decay modes are the decays to the sneutrinos and the decay $\chi_1^\pm \rightarrow \chi_1^0 W$ which tends to dominate when kinematically allowed. As Λ increases above 30 TeV, the masses of the heavier sleptons ($\tilde{\tau}_2$, $\tilde{\mu}_2$ and \tilde{e}_2) fall below the mass of the chargino and so the decays to these heavier sleptons are allowed as well.

For the second lightest neutralino, there are again up to 11 main decay modes. At low values of Λ , the decays to the lighter sleptons are dominant with $\chi_2^0 \rightarrow \tilde{\tau}_1\tau$ having a slight edge over the other two slepton decays. As Λ increases the decays to the sneutrinos gradually become more important. In addition the decay $\chi_2^0 \rightarrow \chi_1^0 h$ and the decays to the heavier sleptons become kinematically allowed and dominate over the other decays.

In chargino pair production at low values of Λ , two τ leptons are always produced because essentially the only decay mode for the chargino is $\chi_1^\pm \rightarrow \tilde{\tau}_1\nu_\tau$ while the stau decays

via $\tilde{\tau}_1 \rightarrow \tau \tilde{G}$. On the other hand, the classic three τ signature for $\chi_2^0 \chi_1^\pm$ production will be diminished since $\chi_2^0 \rightarrow \tilde{\tau}_1 \tau$, $\chi_2^0 \rightarrow \tilde{\mu}_1 \mu$ and $\chi_2^0 \rightarrow \tilde{e}_1 e$ are all roughly equal. Since the subsequent decays of the selectron and smuon to the gravitino produces no τ leptons (unlike the three-body decay modes $\tilde{e}_1 \rightarrow e \tau \tilde{\tau}_1$ and $\tilde{\mu}_1 \rightarrow \mu \tau \tilde{\tau}_1$ that were dominant in the other two cases), there will tend to be a depletion in τ -jets here relative to the previous type 2 case which didn't satisfy the co-NLSP condition. For larger values of Λ , the situation is more complicated, but the decay will frequently involve the lightest neutralino. The lightest neutralino in turn tends to decay to $\tilde{\tau}_1$, $\tilde{\mu}_1$ and \tilde{e}_1 roughly equally. Thus there is again a relative depletion in events with τ -jets.

The E_T distribution for the leading τ -jet when $\Lambda = 25$ TeV is given in Fig. 17. The E_T distribution of the secondary τ -jet is given in Fig. 18. Qualitatively, these are much the same as in the previous cases. At $\Lambda = 25$ TeV, the decay chains are relatively short and the τ -jets tend to be quite hard. The \cancel{E}_T distribution is given in Fig. 19.

We now consider the details of the various final state possibilities. Table IX gives the inclusive branching ratios for different numbers of τ -jets for $\Lambda = 25$ TeV. With $\chi_1^\pm \rightarrow \tilde{\tau}_1 \nu_\tau$ being the only decay mode here, $\chi_1^+ \chi_1^-$ production produces two τ leptons. Thus the probability for τ -jets before cuts is dictated by the hadronic branching ratio of the τ lepton. Including cuts diminishes the number of events with a given number of τ -jets. For example, the branching ratio for 2 τ -jets falls from 42% to 10.5%. When Λ is increased, the situation changes dramatically. Table X gives the inclusive branching ratios for $\Lambda = 40$ TeV. The possibility exists to create many τ -jets, but the probability for creating more than three is low. In addition, the probability for producing no τ -jets is high at $\sim 35\%$. After cuts, the only appreciable modes are the two τ -jets mode at 10% and the one τ -jet mode at 18%.

Turning now to $\chi_2^0 \chi_1^\pm$ production, we see that at low Λ , there is the potential to produce up to three τ -jets. The rates are diminished by the strong presence of $\chi_2^0 \rightarrow \tilde{e}_1 e$ and $\chi_2^0 \rightarrow \tilde{\mu}_1 \mu$, however, and the rate for no τ -jets is high at $\sim 25\%$. After cuts, the two τ -jets branching ratio is only about 7% and the one τ -jet rate is about 25%. For $\Lambda = 40$ TeV, the potential exists to create many more τ -jets, but the one and two τ -jets modes remain dominant with after cuts branching ratios of 19% and 11%, respectively.

For $\tilde{\tau}_1^+ \tilde{\tau}_1^-$, the situation is pretty much the same as it is in the previous cases considered. With $\tilde{\tau}_1 \rightarrow \tau \tilde{G}$ being the only decay mode of the lighter stau, the probability for a given number of τ -jets is completely dictated by the hadronic branching ratio of the τ lepton. The branching ratios after cuts are largely dictated by the mass of the stau.

We now consider the possibility of observing these events at the Tevatron's Run II and TeV33. Fig. 20 shows the combined production rates for the inclusive τ -jet modes before cuts for all the SUSY production modes considered. We do not include the cross sections for more than three τ -jets as these are prohibitively small. In sharp contrast to the previous cases, the most typical situation is that no τ -jets are produced. For low values of Λ ($\Lambda < 40$ TeV), however, the production rates for one and two τ -jets are comparable. The results after cuts are shown in Fig. 21. The one τ -jet mode is dominant and the two τ -jet mode is respectably high. For $\Lambda = 25$ TeV, the two τ -jets rate is about 28 fb which gives about 56 events for 2 fb^{-1} of data and 840 events for 30 fb^{-1} of data. For $\Lambda = 40$ TeV, we have a lower production rate of 1.8 fb. For 2 fb^{-1} of data this corresponds to ~ 4 events, while 30 fb^{-1} of data gives about 54 events.

The branching ratios for some of the more important individual modes are given in

Table XII. Unlike the previous cases considered, there is the potential that modes with specific numbers of charged leptons could be important. We see from the table that for $\Lambda = 25 \text{ TeV}$, the rate for an electron and a τ -jet is 12.7 fb after cuts. For electrons and muons combined, this is 25.4 fb . For an integrated luminosity of 2 fb^{-1} , this corresponds to about 50 events, while for an integrated luminosity of 30 fb^{-1} , this corresponds to about 762 events. A better signal is the $2 e + \tau$ -jet and $2 \mu + \tau$ -jet signals. The combined cross section for this is 13 fb . For 2 fb^{-1} of data, this corresponds to 26 events. For 30 fb^{-1} of data, this corresponds to about 390 events.

VII. CONCLUSION

We have considered the phenomenology of GMSB models where the lighter stau is the NLSP and decays promptly. We have looked at a wide range of the GMSB parameter space. Typically, in those regions of the parameter space where SUSY production can occur at an observable rate, the dominant SUSY production modes are $\chi_1^+ \chi_1^-$ and $\chi_2^0 \chi_1^\pm$, although slepton pair production can be significant in those regions of the parameter space where χ_1^\pm and χ_2^0 are too massive to be readily produced. The decays of the SUSY particles lead to events containing two or three τ leptons plus large missing transverse energy. Searching for the τ lepton signals by the hadronic decays of the τ leptons to thin jets is complicated by the fact that, while primary τ -jets can have high E_T , the secondary τ -jets tend to be rather soft. As a result, many of the τ -jets tend to be eliminated by the cuts. We've shown that the most promising channel is the two τ -jets mode, while the three τ -jets mode can be important at the higher integrated luminosity at Run III. This τ -jet is degraded in the co-NLSP case where the lighter charged sleptons are nearly degenerate in mass. The missing transverse energy associated with the events is large providing a good trigger for these events. Good τ identification will be extremely important to detect the signal.

ACKNOWLEDGMENTS

We thank B. Dutta and G. Wolf for many helpful discussions and S. P. Martin for some useful correspondence. This research was supported by U.S. Department of Energy Grant No. DE-FG03-98ER41076.

REFERENCES

- [1] M. Dine and A. Nelson, Phys. Rev. D **47**, 1277 (1993); M. Dine, A. Nelson and Y. Shirman, Phys. Rev. D **51**, 1362 (1995); M. Dine, A. Nelson, Y. Nir and Y. Shirman, Phys. Rev. D **53**, 2658 (1996); M. Dine, Y. Nir and Y. Shirman, Phys. Rev. D **55**, 1501 (1997).
- [2] I. Affleck, M. Dine and N. Seiberg, Nucl. Phys. **B256**, 557 (1997); R. N. Mohapatra and S. Nandi, Phys. Rev. Lett. **79**, 181 (1997); B. Dobrescu, Phys. Lett. B **403**, 285, (1997); Z. Chacko, B. Dutta, R. N. Mohapatra and S. Nandi, Phys. Rev. D **56**, 5466 (1997).
- [3] G.F. Giudice and R. Rattazzi, hep-ph/9801271; S. Dimopoulos, S. Thomas and J. D. Wells, Nucl. Phys. **B488**, 39 (1997); J. Bagger, D. Pierce, K. Matchev and R.-J. Zhang, Phys. Rev. D **55**, 3188 (1997); K. S. Babu, C. Kolda and F. Wilczek, Phys. Rev. Lett. **77**, 3070 (1996); S. Ambrosanio, G. L. Kane, G. D. Kribs, S. P. Martin and S. Mrenna, Phys. Rev. D **54**, 5395 (1996); *ibid.*, Phys. Rev. D **55**, 1372 (1997); H. Baer, M. Brhlik, C.-H. Chen and X. Tata, Phys. Rev. D **56**, 4463 (1997); D. A. Dicus, B. Dutta and S. Nandi, Phys. Rev. Lett. **78**, 3055 (1997); Phys. Rev. D **56**, 5748, (1997); K. Cheung, D. A. Dicus, B. Dutta and S. Nandi, hep-ph/9711216; A. Riotto, O. Tornkvist and R. N. Mohapatra, Phys. Lett. **B388**, 599 (1996); G. Bhattacharyya, A. Romanino; Phys. Rev. D **55**, 7015 (1997); A. Datta, A. Kundu, B. Mukhopadhyaya and S. Roy, Phys. Lett. **B416**, 117 (1998); Y. Nomura, K. Tobe, hep-ph/9708377, S. Raby and K. Tobe, 9805317; S. Raby, hep-ph/9712254; S. P. Martin and J. D. Wells, hep-ph/9805289.
- [4] S. Dimopoulos, M. Dine, S. Raby and S. Thomas, Phys. Rev. Lett. **76**, 3494 (1996); S. Ambrosanio, G. L. Kane, G. D. Kribs, S. P. Martin and S. Mrenna, Phys. Rev. Lett. **76**, 3498 (1996); D. R. Stump, M. Wiest and C.P. Yuan, Phys. Rev. D **54**, 1936 (1996).
- [5] B. Dutta, D. Muller and S. Nandi, hep-ph/9807390; B. Dutta and S. Nandi, hep-ph/9709511; J. L. Feng and T. Moroi, hep-ph/9712499.
- [6] N. G. Deshpande, B. Dutta and S. Oh, Phys. Rev. D **56** 519 (1997); R. Rattazzi and U. Sarid, hep-ph/9612464.
- [7] S. Dimopoulos, G. F. Giudice and A. Pomarol, Phys. Lett. B **389**, 37 (1996); S. P. Martin, Phys. Rev. D **55**, 3177 (1997).
- [8] V. Barger, M. S. Berger, and P. Ohmann, Phys. Rev. D **49**, 4908 (1994). Our sign convention for μ is the same as in this paper.
- [9] S. Ambrosanio, G. D. Kribs and S. P. Martin, Phys. Rev. D **56**, 1761 (1997).
- [10] P. P. Bagley *et al.*, in *Proceedings of the 1996 DPF/DPB Summer Study on New Directions for High Energy Physics (Snowmass '96)*, Snowmass, CO, June 25-July 12, 1996; D. Amidei *et al.*, unpublished TeV33 Committee report, available at <http://www-theory.fnal.gov/tev33.ps>.
- [11] S. Ambrosanio, G. D. Kribs and S. P. Martin, Nucl. Phys. **B516**, 55 (1998).
- [12] G. Wolf, Talk at the *29th International Conference on High Energy Physics*, Vancouver, Canada, July 23-29, 1998; A. Galloni, DELPHI Collaboration, Talk at "The pheno-CTEQ Symposium 98-Frontiers of Phenomenology", Madison, Wisconsin March 23-26, 1998; V. Büscher, ALEPH Collaboration, Talk at Fermilab, July 10, 1998, http://alephwww.cern.ch/~buescher/w_c/talk.ps.

TABLES

TABLE I. Branching ratios of the sparticles of interest for the parameters $n = 2$, $\tan \beta = 15$ and $M/\Lambda = 3$. The decays of the $\tilde{\mu}_1$ are obtained by replacing the e with a μ in the \tilde{e}_1 decays.

Decay Mode	Λ (TeV)						
	35	40	50	60	70	80	85
$\chi_1^\pm \rightarrow \tilde{\tau}_1 \nu_\tau$	1	1	0.6787	0.5192	0.4440	0.3996	0.3833
$\chi_1^\pm \rightarrow \chi_1^0 W$	-	-	0.3213	0.4808	0.5560	0.6004	0.6167
$\chi_2^0 \rightarrow \tilde{\tau}_1 \tau$	0.5677	0.5965	0.6235	0.3075	0.2137	0.1719	0.1578
$\chi_2^0 \rightarrow \tilde{\mu}_1 \mu$	0.2162	0.2017	0.1660	0.0659	0.0378	0.0256	0.0217
$\chi_2^0 \rightarrow \tilde{e}_1 e$	0.2162	0.2017	0.1660	0.0659	0.0378	0.0256	0.0217
$\chi_2^0 \rightarrow \chi_1^0 Z$	-	-	0.0446	0.0318	0.0251	0.0219	0.0207
$\chi_2^0 \rightarrow \chi_1^0 h$	-	-	-	0.5289	0.6856	0.7550	0.7780
$\chi_1^0 \rightarrow \tilde{\tau}_1 \tau$	1	1	0.8577	0.6542	0.5659	0.5215	0.5072
$\chi_1^0 \rightarrow \tilde{\mu}_1 \mu$	-	-	0.0711	0.1729	0.2170	0.2392	0.2464
$\chi_1^0 \rightarrow \tilde{e}_1 e$	-	-	0.0711	0.1729	0.2170	0.2392	0.2464
$\tilde{e}_1 \rightarrow \chi_1^0 e$	1	1	-	-	-	-	-
$\tilde{e}_1^- \rightarrow e^- \tau^- \tilde{\tau}^+$	-	-	0.5205	0.5287	0.5315	0.5310	0.5298
$\tilde{e}_1^- \rightarrow e^- \tau^+ \tilde{\tau}^-$	-	-	0.4795	0.4697	0.4634	0.4580	0.4554
$\tilde{e}_1 \rightarrow e \tilde{G}$	-	-	-	0.0016	0.0050	0.0110	0.0148

TABLE II. Inclusive tau-jet branching ratios for the dominant production mechanisms for the parameters $n = 2$, $\tan \beta = 15$, $\Lambda = 35$ TeV and $M = 105$ TeV.

Production Mode	1 τ -jet	2 τ -jets	3 τ -jets	4 τ -jets	5 τ -jets
$\chi_1^+ \chi_1^-$: no cuts	0.4562	0.4200	-	-	-
with cuts	0.2577	0.1084	-	-	-
$\chi_1^\pm \chi_2^0$: no cuts	0.2408	0.4434	0.2723	-	-
with cuts	0.2558	0.1567	0.0259	-	-
$\tilde{\tau}_1^+ \tilde{\tau}_1^-$: no cuts	0.4560	0.4203	-	-	-
with cuts	0.2523	0.0939	-	-	-
$\tilde{e}_1^+ \tilde{e}_1^-$: no cuts	0.1128	0.3118	0.3834	0.1766	-
with cuts	0.2383	0.0778	0.0003	<i>negl.</i>	-

TABLE III. Inclusive tau-jet branching ratios for the dominant production mechanisms for the parameters $n = 2$, $\tan \beta = 15$, $\Lambda = 50$ TeV and $M = 150$ TeV.

Production Mode	1 τ -jet	2 τ -jets	3 τ -jets	4 τ -jets	5 τ -jets
$\chi_1^+ \chi_1^-$: no cuts	0.3194	0.4099	0.1627	0.0291	0.0027
with cuts	0.3355	0.1610	0.0100	0.0004	<i>negl.</i>
$\chi_1^\pm \chi_2^0$: no cuts	0.1969	0.3961	0.3060	0.0626	0.0044
with cuts	0.3234	0.2238	0.0472	0.0014	<i>negl.</i>
$\tilde{\tau}_1^+ \tilde{\tau}_1^-$: no cuts	0.4561	0.4201	-	-	-
with cuts	0.3345	0.1370	-	-	-
$\tilde{e}_1^+ \tilde{e}_1^-$: no cuts	0.1130	0.3119	0.3833	0.1765	-
with cuts	0.3199	0.1207	0.0023	<i>negl.</i>	-

TABLE IV. Inclusive tau-jet branching ratios for the dominant production mechanisms for the parameters $n = 2$, $\tan \beta = 15$, $\Lambda = 70$ TeV and $M = 210$ TeV.

Production Mode	1 τ -jet	2 τ -jets	3 τ -jets	4 τ -jets	5 τ -jets
$\chi_1^+ \chi_1^-$: no cuts	0.2333	0.3821	0.2549	0.0728	0.0078
with cuts	0.3647	0.2119	0.0322	0.0023	<i>negl.</i>
$\chi_1^\pm \chi_2^0$: no cuts	0.1574	0.3455	0.3259	0.1210	0.0202
with cuts	0.3419	0.2334	0.0569	0.0071	0.0008
$\tilde{\tau}_1^+ \tilde{\tau}_1^-$: no cuts	0.4561	0.4201	-	-	-
with cuts	0.3988	0.1711	-	-	-
$\tilde{e}_1^+ \tilde{e}_1^-$: no cuts	0.1165	0.3133	0.3795	0.1743	-
with cuts	0.3901	0.1495	0.0013	<i>negl.</i>	-

TABLE V. Production rates in fb for some of the more interesting final state configurations with and without cuts for the parameters $n = 2$, $\tan \beta = 15$ and $M/\Lambda = 3$.

	$\Lambda = 35$ TeV		$\Lambda = 50$ TeV	
	no cuts	cuts	no cuts	cuts
1 τ -jet	-	51.17	-	3.71
$e/\mu + 1$ τ -jet	85.44	11.91	4.98	1.59
1 jet + 1 τ -jet	-	21.58	-	2.36
2 jets + 1 τ -jet	-	-	-	2.35
$e/\mu + 2$ jets + 1 τ -jet	-	-	-	0.69
2 τ -jets	157.3	40.64	9.18	3.91

TABLE VI. Branching ratios of some of the sparticles of interest for the parameter set with $n = 3$, $\tan \beta = 15$ and $M/\Lambda = 20$.

Decay Mode	Λ (TeV)				
	25	30	40	50	55
$\chi_1^\pm \rightarrow \tilde{\tau}_1 \nu_\tau$	0.8062	0.6330	0.3514	0.2211	0.1839
$\chi_1^\pm \rightarrow \tilde{\tau}_2 \nu_\tau$	-	-	0.0118	0.0493	0.0643
$\chi_1^\pm \rightarrow \tilde{e}_2 \nu_e$	-	-	0.023	0.061	0.074
$\chi_1^\pm \rightarrow \tilde{\nu}_\tau \tau$	0.0729	0.1097	0.1379	0.1450	0.1467
$\chi_1^\pm \rightarrow \tilde{\nu}_e e$	0.0604	0.0954	0.1253	0.1342	0.1365
$\chi_1^\pm \rightarrow \chi_1^0 W$	-	0.0666	0.2022	0.1943	0.1832
$\chi_2^0 \rightarrow \tilde{\tau}_1 \tau$	0.5760	0.5653	0.2894	0.1678	0.1385
$\chi_2^0 \rightarrow \tilde{\tau}_2 \tau$	-	-	0.0142	0.0432	0.0542
$\chi_2^0 \rightarrow \tilde{e}_1 e$	0.1667	0.1335	0.0478	0.0207	0.0151
$\chi_2^0 \rightarrow \tilde{e}_2 e$	-	-	0.0240	0.0507	0.0602
$\chi_2^0 \rightarrow \tilde{\nu}_\tau \nu_\tau$	0.0317	0.0583	0.0760	0.0811	0.0845
$\chi_2^0 \rightarrow \tilde{\nu}_e \nu_e$	0.0294	0.0547	0.0722	0.07764	0.0810
$\chi_2^0 \rightarrow \chi_1^0 Z$	-	-	0.0196	0.0136	0.0119
$\chi_2^0 \rightarrow \chi_1^0 h$	-	-	0.3127	0.3961	0.3983
$\chi_1^0 \rightarrow \tilde{\tau}_1 \tau$	0.7955	0.6011	0.4707	0.4268	0.4150
$\chi_1^0 \rightarrow \tilde{e}_1 e$	0.1023	0.1994	0.2646	0.2866	0.2925
$\tilde{e}^- \rightarrow e^- \tau^- \tilde{\tau}^+$	0.5563	0.5746	0.5898	0.5960	0.5977
$\tilde{e}^- \rightarrow e^- \tau^+ \tilde{\tau}^-$	0.4437	0.4254	0.4102	0.4040	0.4023

TABLE VII. Inclusive tau-jet branching ratios for the dominant production mechanisms for the parameters $n = 3$, $\tan \beta = 15$, $\Lambda = 25$ TeV and $M = 500$ TeV.

Production Mode	1 τ -jet	2 τ -jets	3 τ -jets	4 τ -jets	5 τ -jets
$\chi_1^+ \chi_1^-$: no cuts	0.3597	0.4040	0.1110	0.0306	0.0033
with cuts	0.2336	0.1138	0.0077	0.0003	<i>negl.</i>
$\chi_1^\pm \chi_2^0$: no cuts	0.2110	0.4077	0.2912	0.0443	0.0085
with cuts	0.2452	0.1682	0.0332	0.0010	<i>negl.</i>
$\tilde{\tau}_1^+ \tilde{\tau}_1^-$: no cuts	0.4555	0.4210	-	-	-
with cuts	0.2258	0.0797	-	-	-
$\tilde{e}_1^+ \tilde{e}_1^-$: no cuts	0.1128	0.3121	0.3833	0.1764	-
with cuts	0.1998	0.0779	0.0063	0.0002	-

TABLE VIII. Inclusive tau-jet branching ratios for the dominant production mechanisms for the parameters $n = 3$, $\tan \beta = 15$, $\Lambda = 40$ TeV and $M = 800$ TeV.

Production Mode	1 τ -jet	2 τ -jet	3 τ -jets	4 τ -jets	5 τ -jets
$\chi_1^+ \chi_1^-$: no cuts	0.1890	0.3484	0.2863	0.1155	0.0223
with cuts	0.3011	0.2123	0.0500	0.0057	0.0003
$\chi_1^\pm \chi_2^0$: no cuts	0.1457	0.3342	0.3301	0.1395	0.0236
with cuts	0.2991	0.2343	0.0672	0.0082	0.0008
$\tilde{\tau}_1^+ \tilde{\tau}_1^-$: no cuts	0.4556	0.4208	-	-	-
with cuts	0.3396	0.1395	-	-	-
$\tilde{e}_1^+ \tilde{e}_1^-$: no cuts	0.1128	0.3121	0.3833	0.1765	-
with cuts	0.3213	0.1270	0.0048	0.0001	-

TABLE IX. Inclusive τ -jet branching ratios for the various production mechanisms for the parameters $n = 3$, $\tan \beta = 3$, $\Lambda = 25$ TeV and $M = 75$ TeV.

Production Mode	1 τ -jet	2 τ -jets	3 τ -jets	4 τ -jets	5 τ -jets
$\chi_1^+ \chi_1^-$: no cuts	0.4562	0.4200	-	-	-
with cuts	0.2514	0.1053	-	-	-
$\chi_1^\pm \chi_2^0$: no cuts	0.5088	0.1514	0.0935	-	-
with cuts	0.2480	0.0666	0.0153	-	-
$\tilde{\tau}_1^+ \tilde{\tau}_1^-$: no cuts	0.4560	0.4203	-	-	-
with cuts	0.2427	0.0891	-	-	-

TABLE X. Inclusive τ -jet branching ratios for the various production mechanisms for the parameters $n = 3$, $\tan \beta = 3$, $\Lambda = 40$ TeV and $M = 120$ TeV.

Production Mode	1 τ -jet	2 τ -jets	3 τ -jets	4 τ -jets	5 τ -jets
$\chi_1^+ \chi_1^-$: no cuts	0.2903	0.2272	0.0937	0.0299	0.0054
with cuts	0.1826	0.0996	0.0227	0.0034	0.0002
$\chi_1^\pm \chi_2^0$: no cuts	0.2613	0.2299	0.0826	0.0298	0.0057
with cuts	0.1903	0.1054	0.0232	0.0038	0.0004
$\tilde{\tau}_1^+ \tilde{\tau}_1^-$: no cuts	0.4560	0.4202	-	-	-
with cuts	0.3419	0.1410	-	-	-

TABLE XI. Branching ratios of some of the sparticles of interest for the parameter set with $n = 3$, $\tan\beta = 3$ and $M/\Lambda = 3$.

Decay Mode	Λ (TeV)					
	25	30	40	50	60	65
$\chi_1^\pm \rightarrow \tilde{\tau}_1 \nu_\tau$	1	0.3416	0.0225	0.0099	0.0063	0.0053
$\chi_1^\pm \rightarrow \tilde{\nu}_\tau \tau$	-	0.2147	0.1426	0.1390	0.1402	0.1410
$\chi_1^\pm \rightarrow \tilde{\nu}_e e$	-	0.2219	0.1418	0.1383	0.1396	0.1405
$\chi_1^\pm \rightarrow \chi_1^0 W$	-	-	0.4514	0.3436	0.2781	0.2552
$\chi_1^\pm \rightarrow \tilde{\tau}_2 \nu_\tau$	-	-	0.0326	0.0765	0.0984	0.1055
$\chi_1^\pm \rightarrow \tilde{e}_2 e$	-	-	0.0336	0.0772	0.0989	0.1060
$\chi_2^0 \rightarrow \tilde{\tau}_1 \tau$	0.3340	0.3135	0.1384	0.0577	0.0302	0.0232
$\chi_2^0 \rightarrow \tilde{e}_1 e$	0.3223	0.2977	0.1265	0.0505	0.0252	0.0190
$\chi_2^0 \rightarrow \tilde{\nu}_\tau \nu_\tau$	0.0071	0.0304	0.0820	0.0987	0.1062	0.1086
$\chi_2^0 \rightarrow \tilde{\nu}_e \nu_e$	0.0071	0.0303	0.0819	0.0986	0.1061	0.1085
$\chi_2^0 \rightarrow \chi_1^0 Z$	-	-	0.0124	0.0083	0.0060	0.0053
$\chi_2^0 \rightarrow \chi_1^0 h$	-	-	0.2146	0.2763	0.2800	0.2779
$\chi_2^0 \rightarrow \tilde{\tau}_2 \tau$	-	-	0.0447	0.0866	0.1049	0.1100
$\chi_2^0 \rightarrow \tilde{e}_2 e$	-	-	0.0456	0.0871	0.1051	0.1101
$\chi_1^0 \rightarrow \tilde{\tau}_1 \tau$	0.3593	0.3437	0.3378	0.3362	0.3355	0.3353
$\chi_1^0 \rightarrow \tilde{e}_1 e$	0.3203	0.3281	0.3311	0.3319	0.3322	0.3323
$\tilde{\nu}_\tau \rightarrow \chi_1^\pm \tau$	0.0047	-	-	-	-	-
$\tilde{\nu}_\tau \rightarrow \nu_\tau \chi_1^0$	0.9953	0.9940	0.9889	0.9875	0.9870	0.9869
$\tilde{\nu}_\tau \rightarrow \tilde{\tau}_1 W$	-	0.0060	0.0111	0.0125	0.0130	0.0131
$\tilde{\nu}_e \rightarrow \chi_1^0 \nu_e$	0.9928	1	1	1	1	1
$\tilde{\nu}_e \rightarrow \chi_1^\pm e$	0.0072	-	-	-	-	-
$\tilde{\tau}_2 \rightarrow \chi_1^0 \tau$	0.4640	0.8960	1	1	1	1
$\tilde{\tau}_2 \rightarrow \chi_1^\pm \nu_\tau$	0.4155	0.0983	-	-	-	-
$\tilde{\tau}_2 \rightarrow \chi_2^0 \tau$	0.1206	0.0057	-	-	-	-
$\tilde{e}_2 \rightarrow \chi_1^0 e$	1	1	1	1	1	1
$\tilde{e}_1 \rightarrow Ge$	1	1	1	1	1	1

TABLE XII. Production rates in fb for some of the more interesting final state configurations with and without cuts for the parameters $n = 3$, $\tan\beta = 3$ and $M/\Lambda = 3$.

	$\Lambda = 25$ TeV		$\Lambda = 30$ TeV	
	no cuts	cuts	no cuts	cuts
τ -jet	-	28.84	-	5.39
2 τ -jets	70.57	23.11	8.01	4.49
e/μ & τ -jet	38.20	12.71	4.35	3.82
$2e/2\mu$ & τ -jet	-	6.48	3.99	2.75

FIGURES

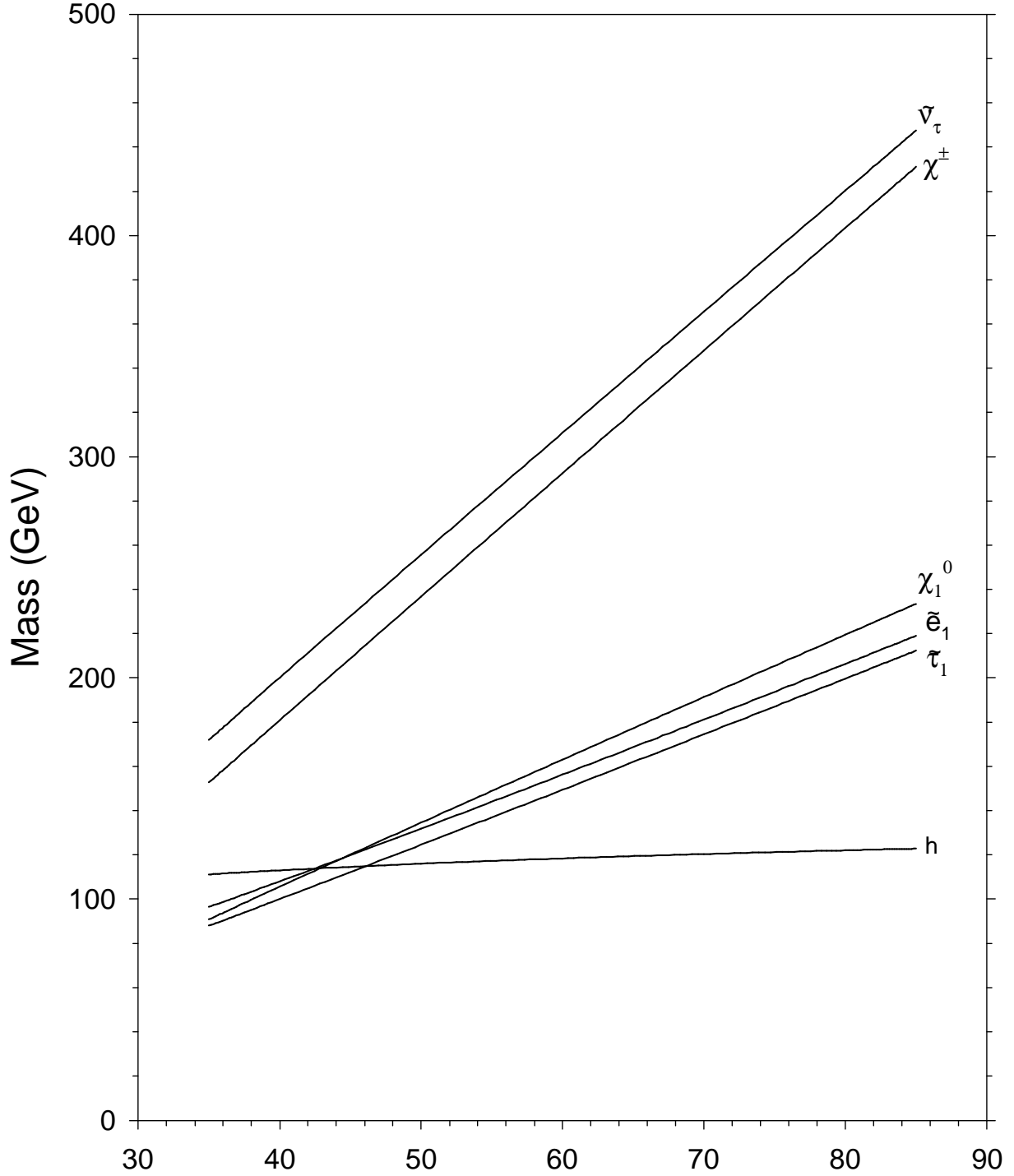


FIG. 1. Masses for the sparticles of interest for the line defined by $n = 2$, $\tan \beta = 15$ and $M/\Lambda = 3$. $M_{\chi_2^0} \approx M_{\chi_1^\pm}$ and $M_{\tilde{\mu}_1} \approx M_{\tilde{e}_1}$.

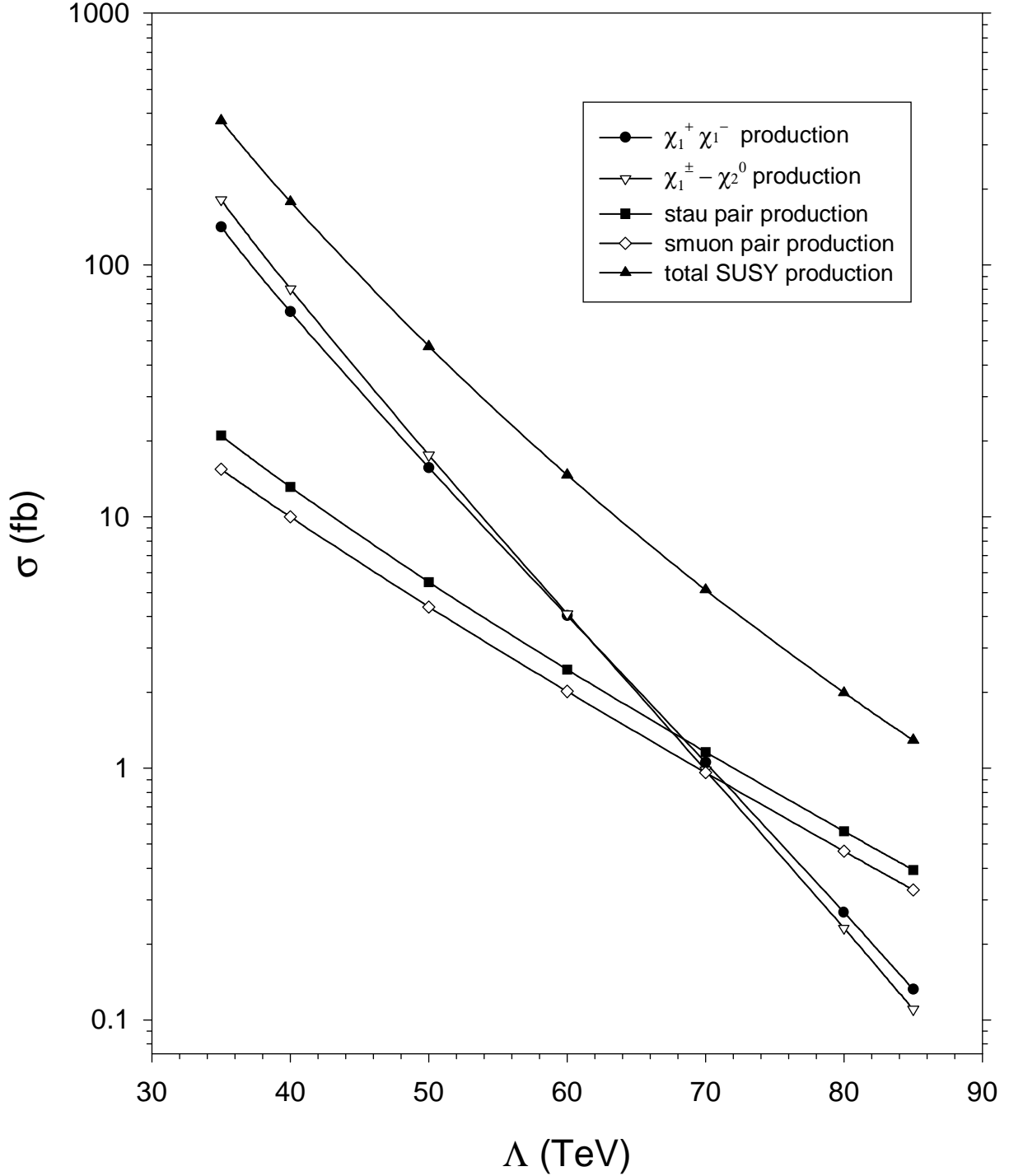


FIG. 2. Cross section for the important SUSY production processes at the Tevatron for the line defined by $n = 2$, $\tan\beta = 15$ and $M/\Lambda = 3$. The $\chi_2^0\chi_1^\pm$ cross section includes production of both signs of the chargino.

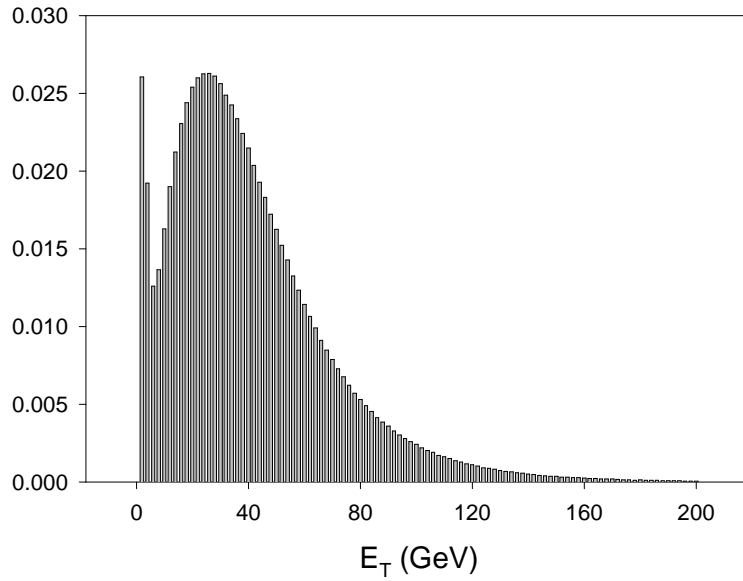
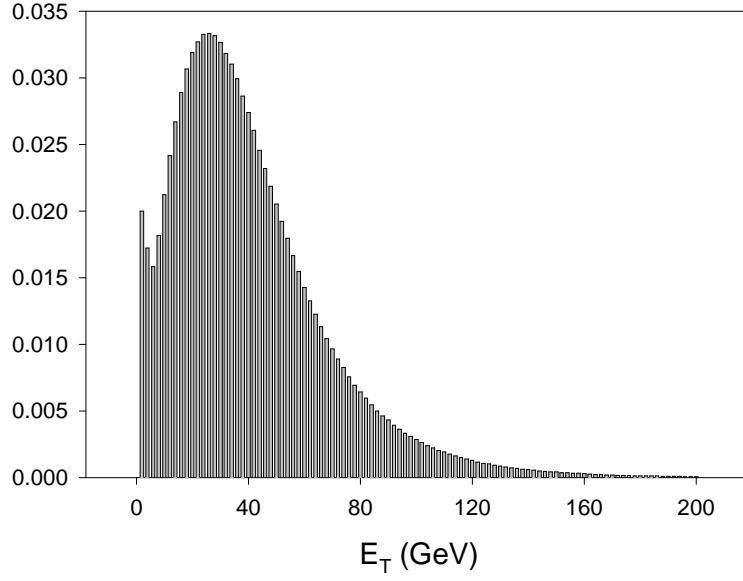
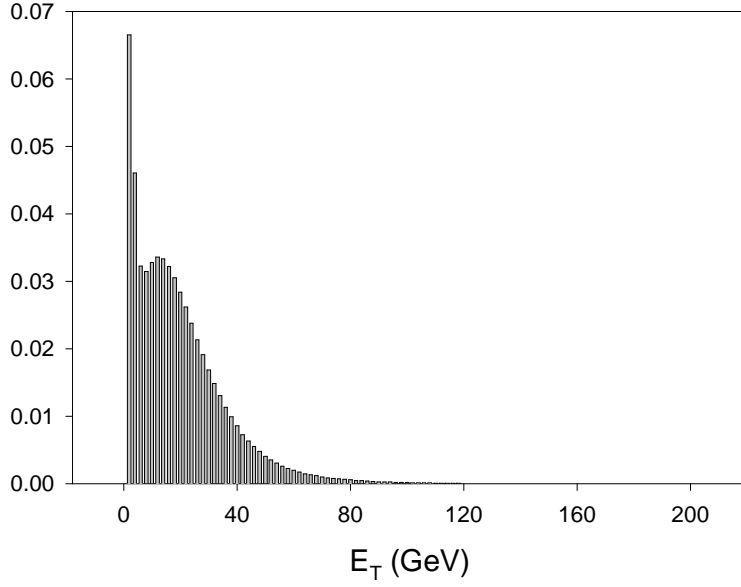
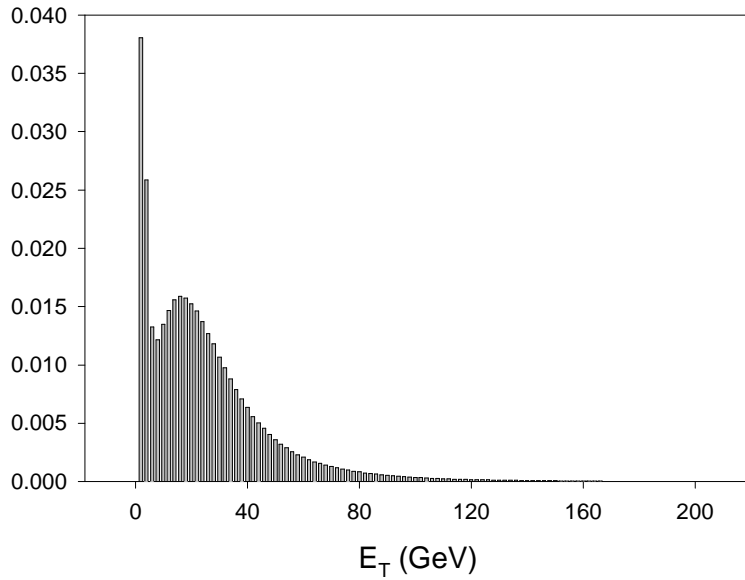


FIG. 3. The E_T distributions of the leading τ jet for the parameters $n = 2$, $\tan \beta = 15$, $M/\Lambda = 3$ and $\Lambda = 35$ TeV. In (a), no cuts have been imposed. In (b), the $|\eta| < 1$ cut has been imposed.

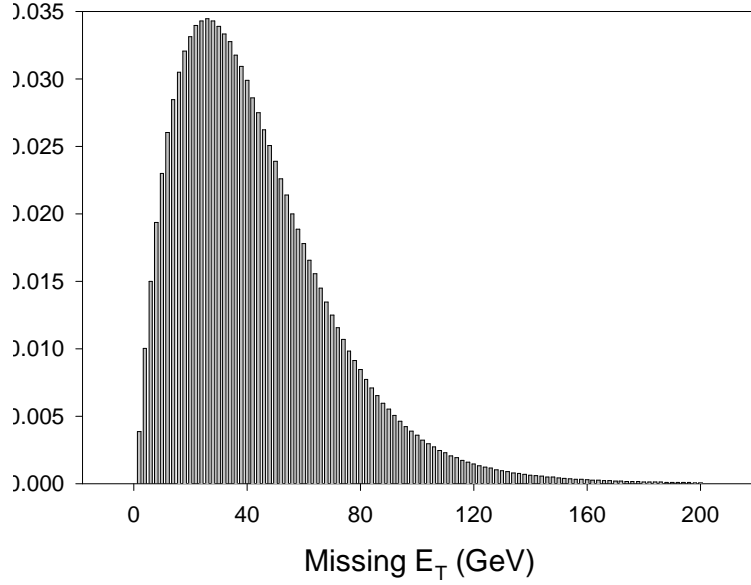


(a)

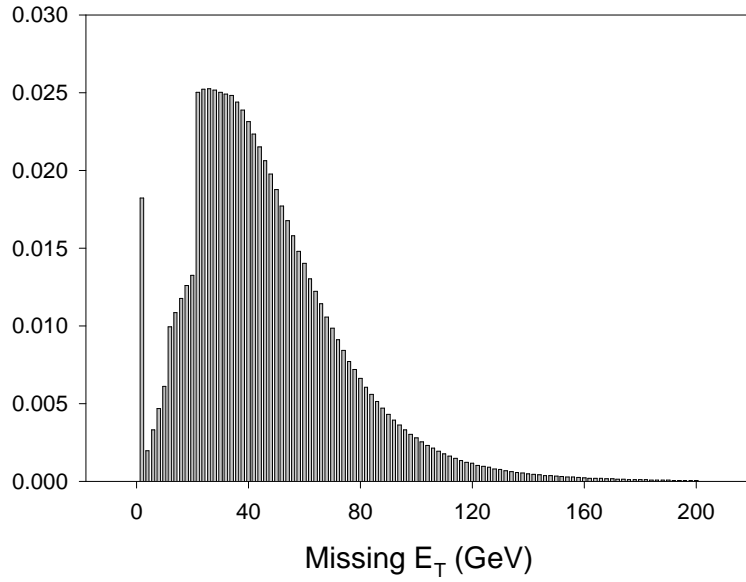


(b)

FIG. 4. The E_T distributions of the secondary τ jet for the parameters $n = 2$, $\tan \beta = 15$, $M/\Lambda = 3$ and $\Lambda = 35$ TeV. In (a), no cuts have been imposed. In (b), the $|\eta| < 1$ cut on τ -jets has been imposed.



(a)



(b)

FIG. 5. \cancel{E}_T distribution of the secondary τ jet for the parameters $n = 2$, $\tan \beta = 15$, $M/\Lambda = 3$ and $\Lambda = 35$ TeV. In (a), no cuts have been imposed. In (b), the E_T/p_T and pseudorapidity cuts on the jets and charged leptons have been imposed.

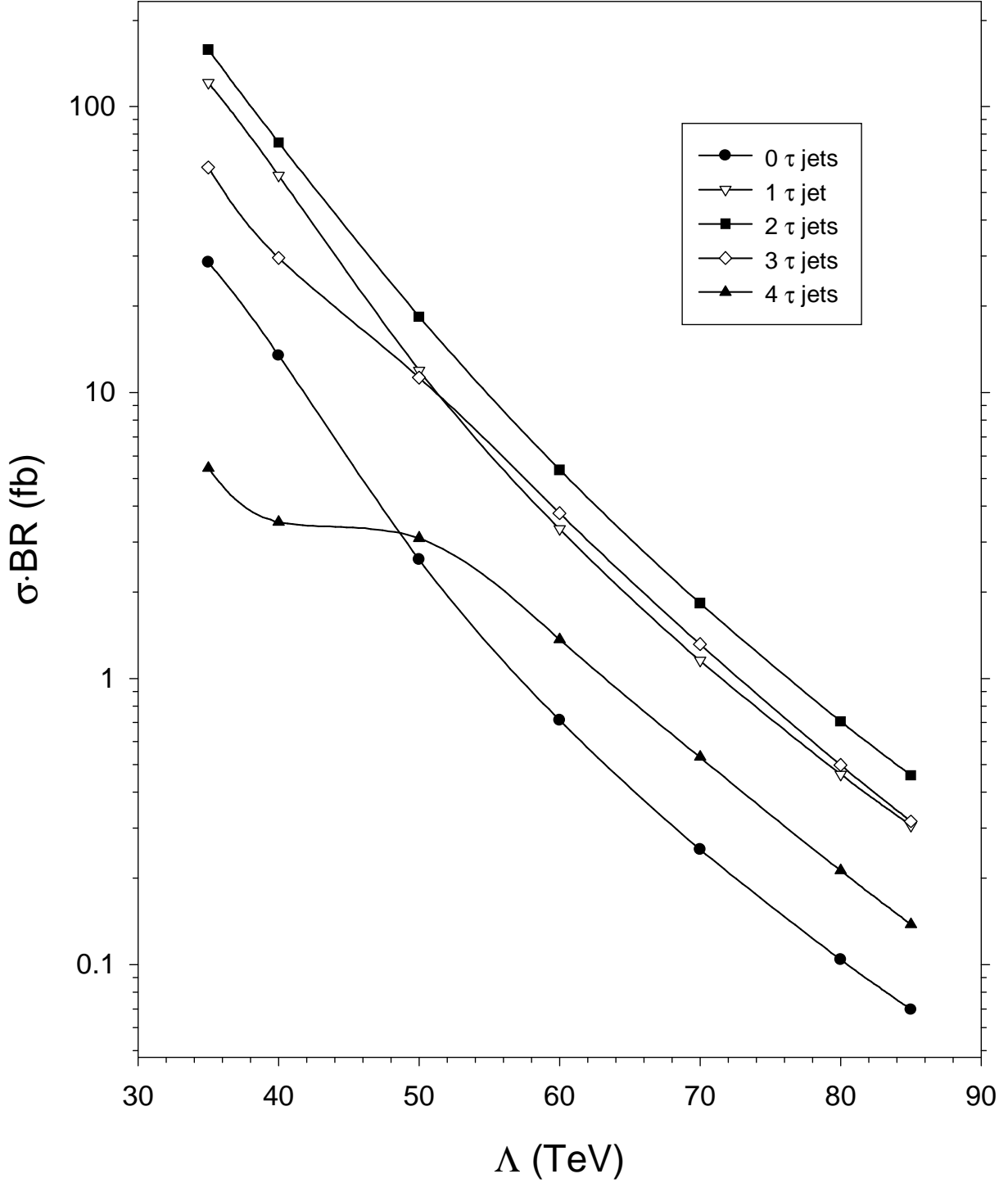


FIG. 6. $\sigma \cdot BR$ before cuts for the inclusive τ jets modes for the parameters $n = 2$, $\tan \beta = 15$ and $M/\Lambda = 3$.

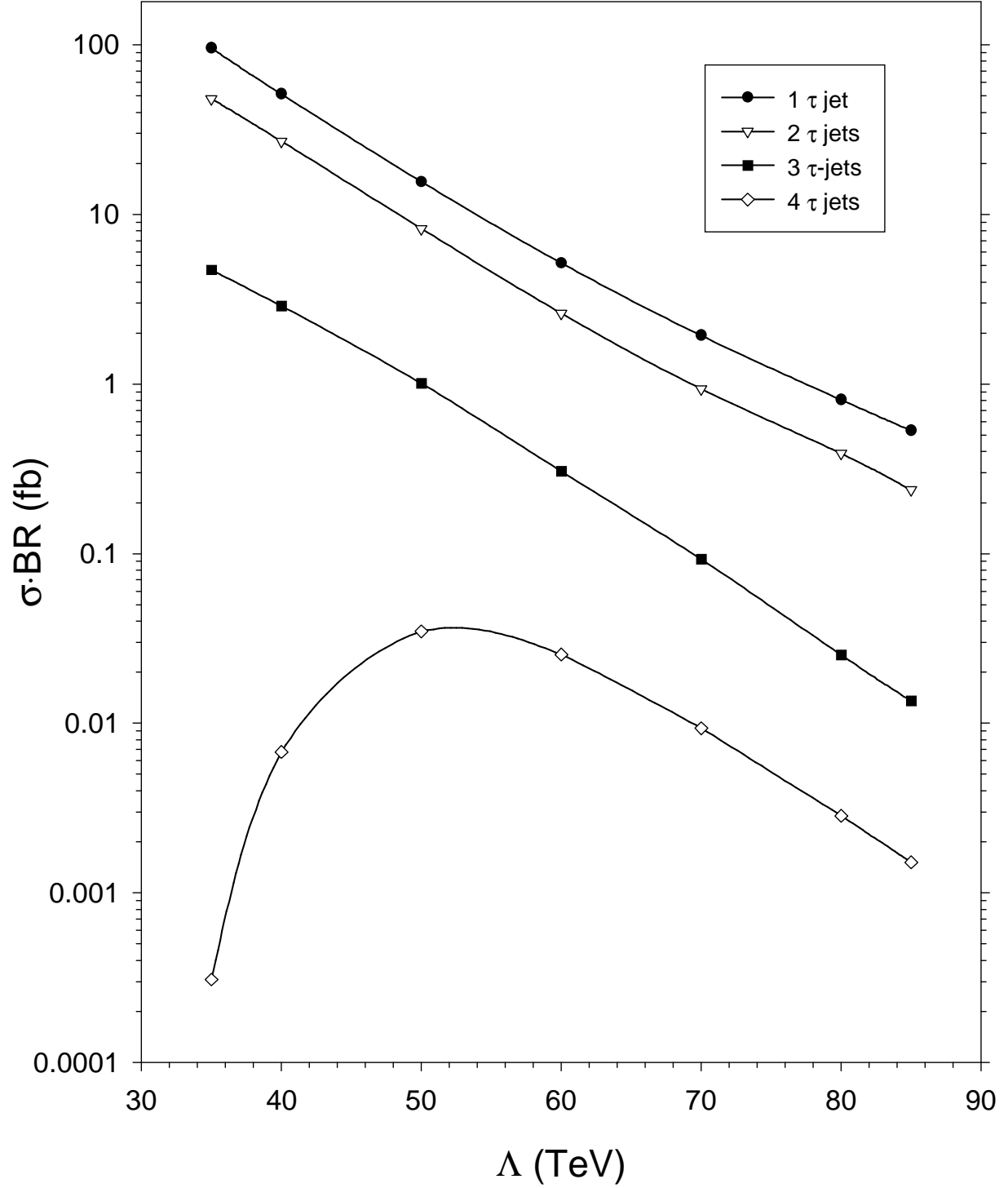


FIG. 7. $\sigma \cdot BR$ after cuts for the inclusive τ jets modes for the parameters $n = 2$, $\tan \beta = 15$ and $M/\Lambda = 3$.

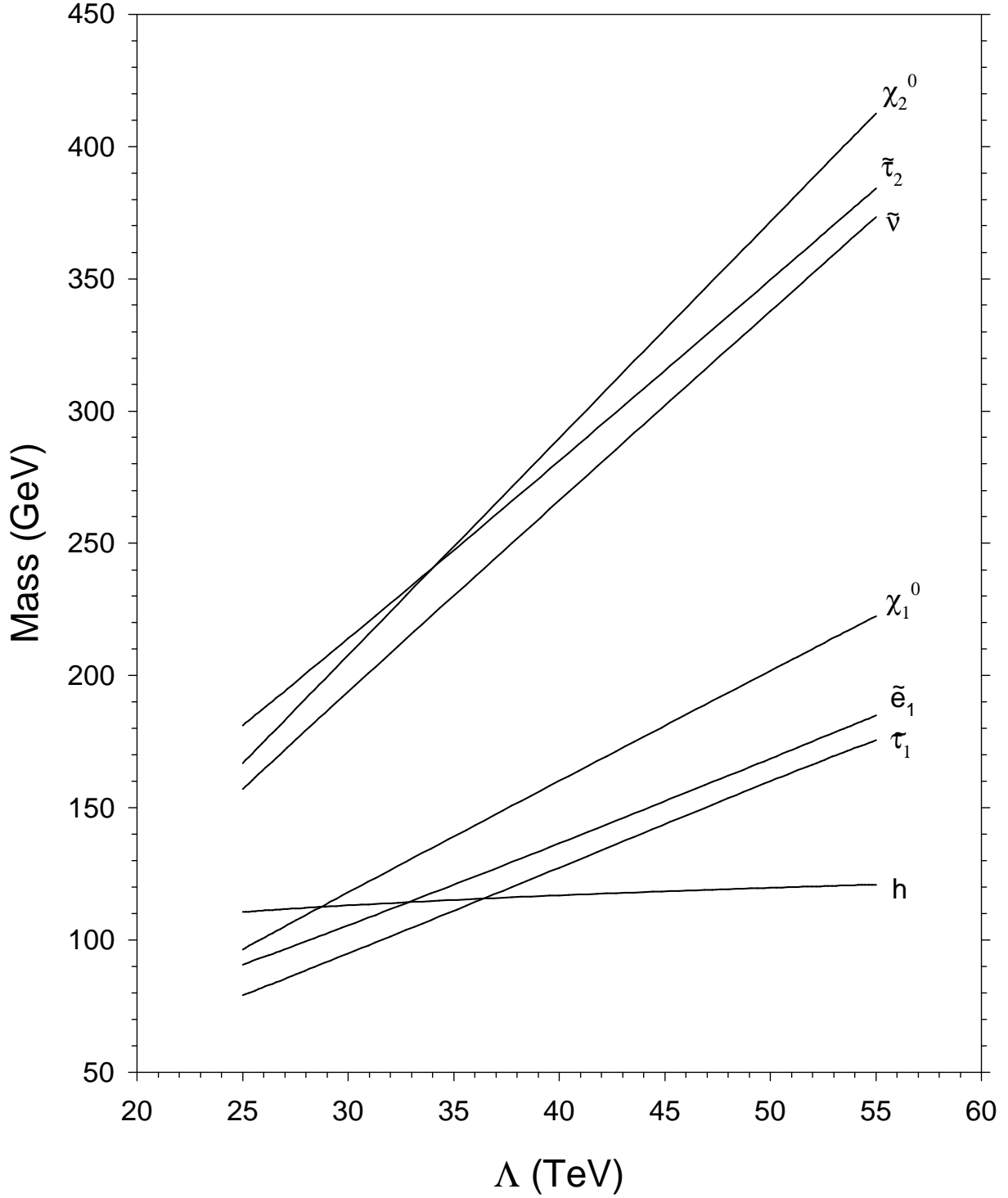


FIG. 8. Masses for the sparticles of interest for the line defined by $n = 3$, $\tan \beta = 15$ and $M/\Lambda = 20$. $M_{\chi_2^0} \approx M_{\chi_1^\pm}$ and $M_{\tilde{\mu}_1} \approx M_{\tilde{e}_1}$.

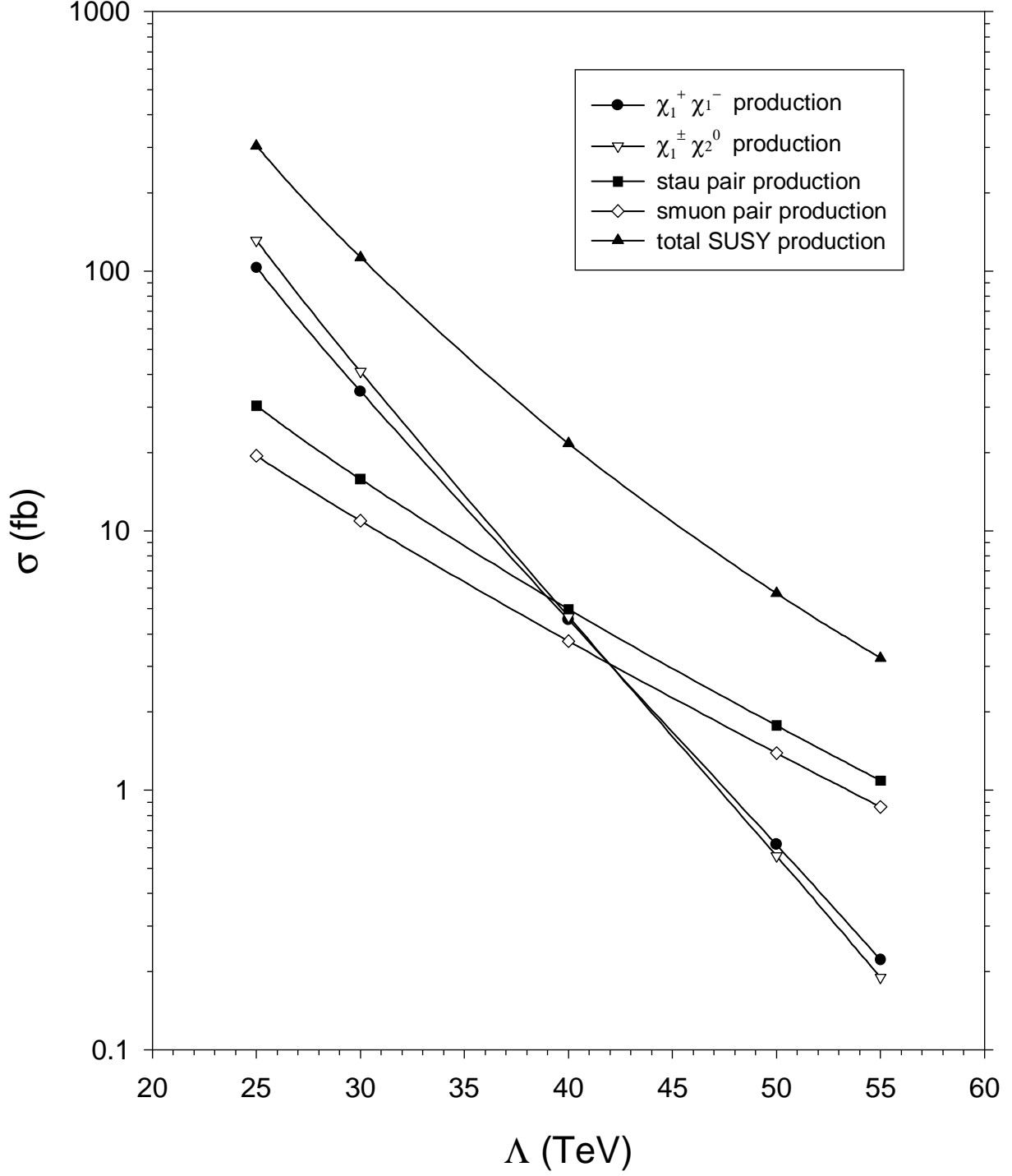
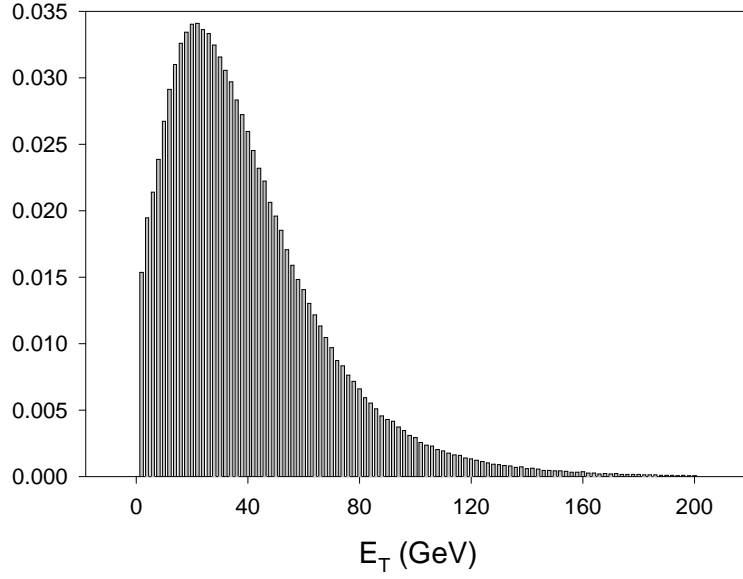
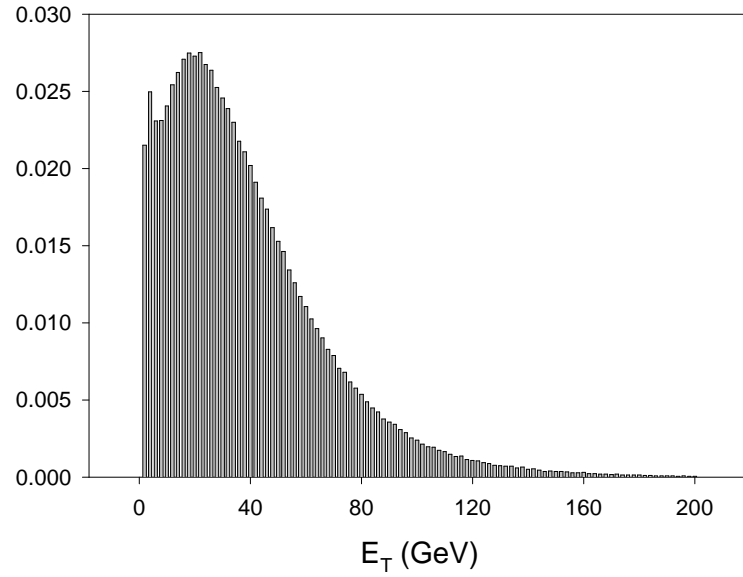


FIG. 9. Cross section for the important SUSY production processes at the Tevatron for the line defined by $n = 3$, $\tan \beta = 15$ and $M/\Lambda = 20$. The $\chi_2^0 \chi_1^\pm$ cross section includes production of both signs of the chargino.

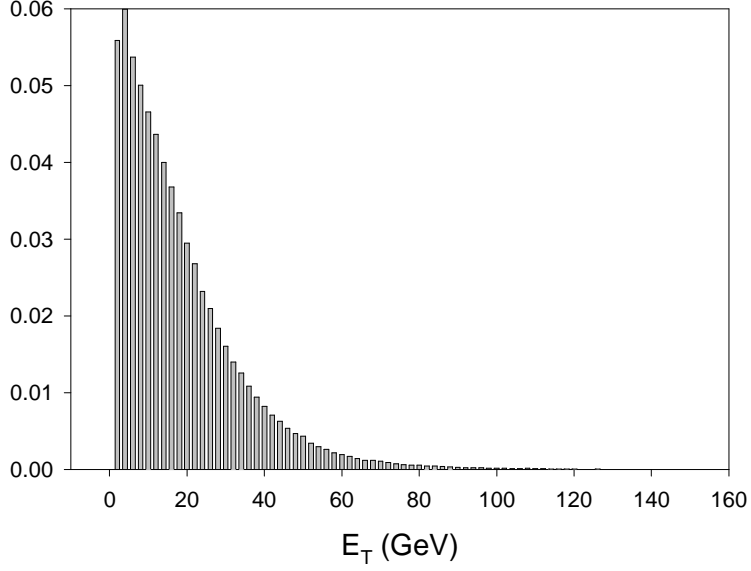


(a)

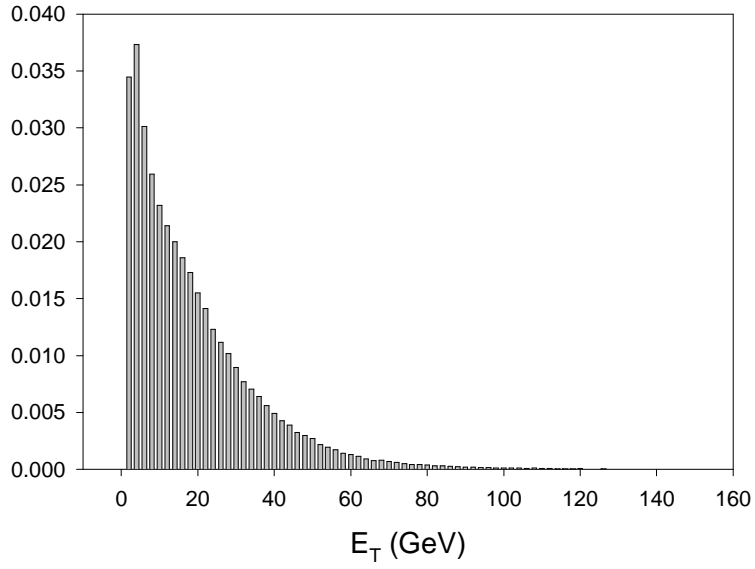


(b)

FIG. 10. The E_T distributions of the leading τ jet for the parameters $n = 3$, $\tan \beta = 15$, $M/\Lambda = 20$ and $\Lambda = 25$ TeV. In (a), no cuts have been imposed. In (b), the $|\eta| < 1$ cut has been imposed on the τ -jets.

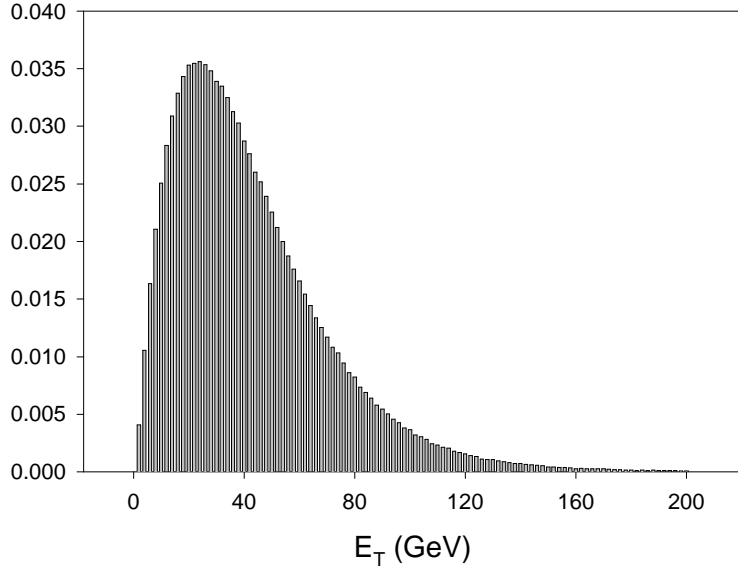


(a)

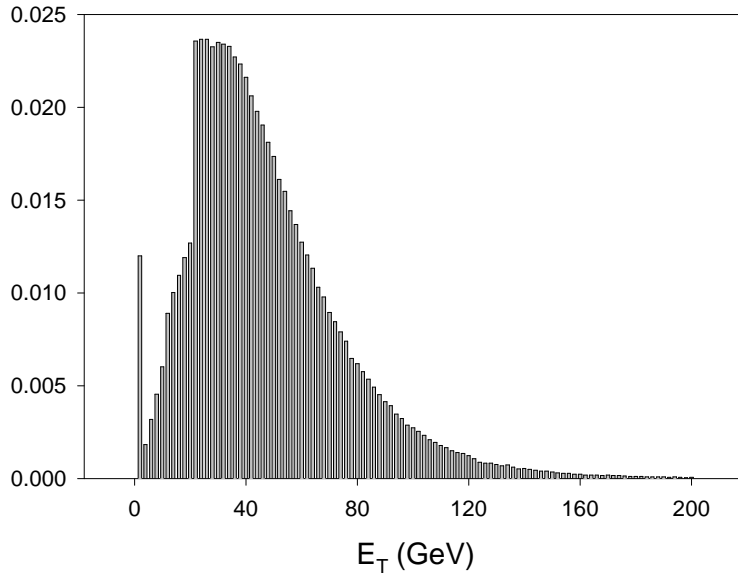


(b)

FIG. 11. The E_T distributions of the secondary τ jet for the parameters $n = 3$, $\tan \beta = 15$, $M/\Lambda = 20$ and $\Lambda = 20$ TeV. In (a), no cuts have been imposed. In (b), $|\eta| < 1$ cut on τ -jets has been imposed.



(a)



(b)

FIG. 12. E_T distribution of the secondary τ jet for the parameters $n = 3$, $\tan \beta = 15$, $M/\Lambda = 20$ and $\Lambda = 25$ TeV. In (a), no cuts have been imposed. In (b), the E_T/p_T and pseudorapidity cuts on the jets and charged leptons have been imposed.

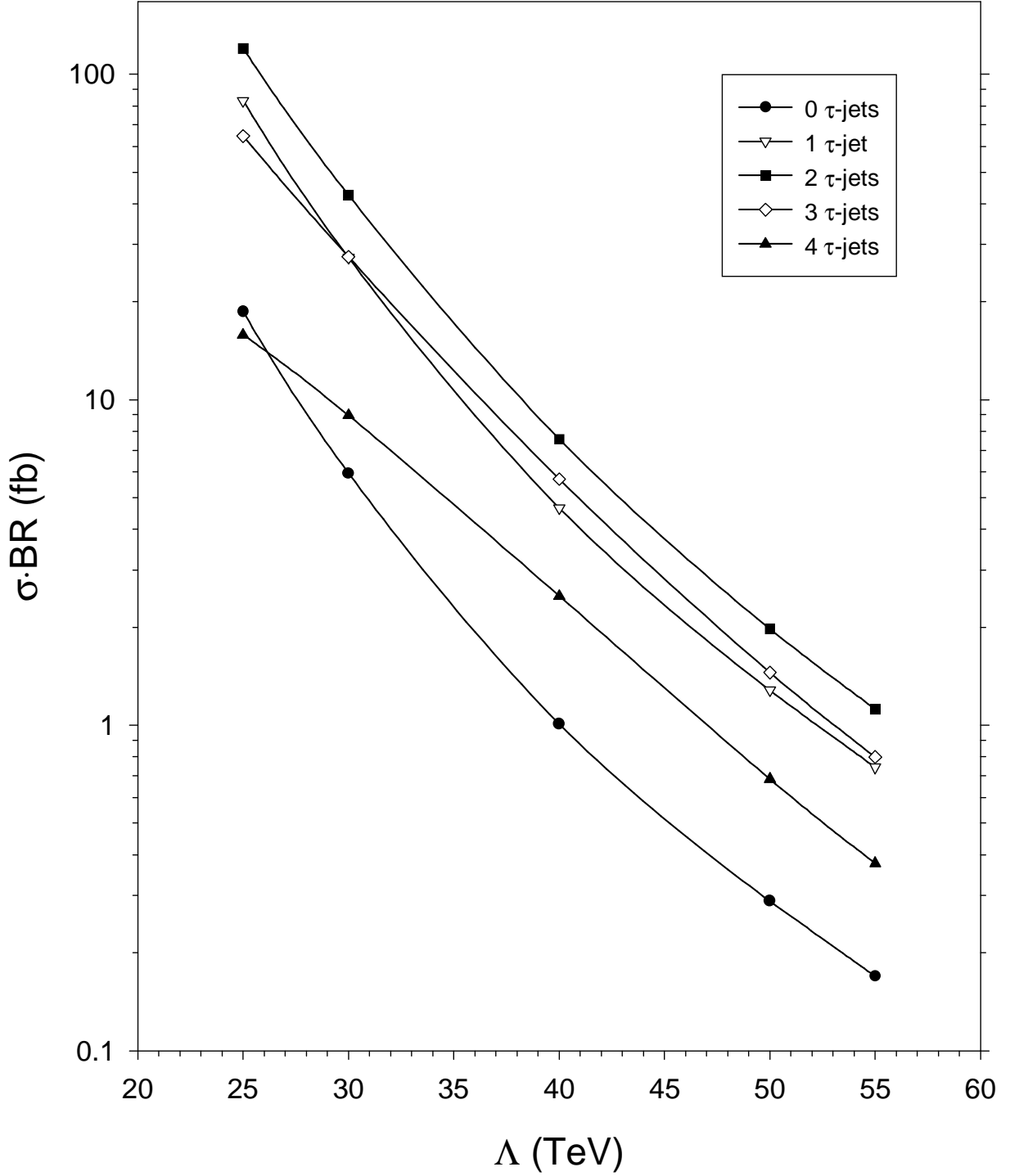


FIG. 13. $\sigma \cdot BR$ before cuts for the inclusive τ jets modes for the parameters $n = 3$, $\tan \beta = 15$ and $M/\Lambda = 20$.

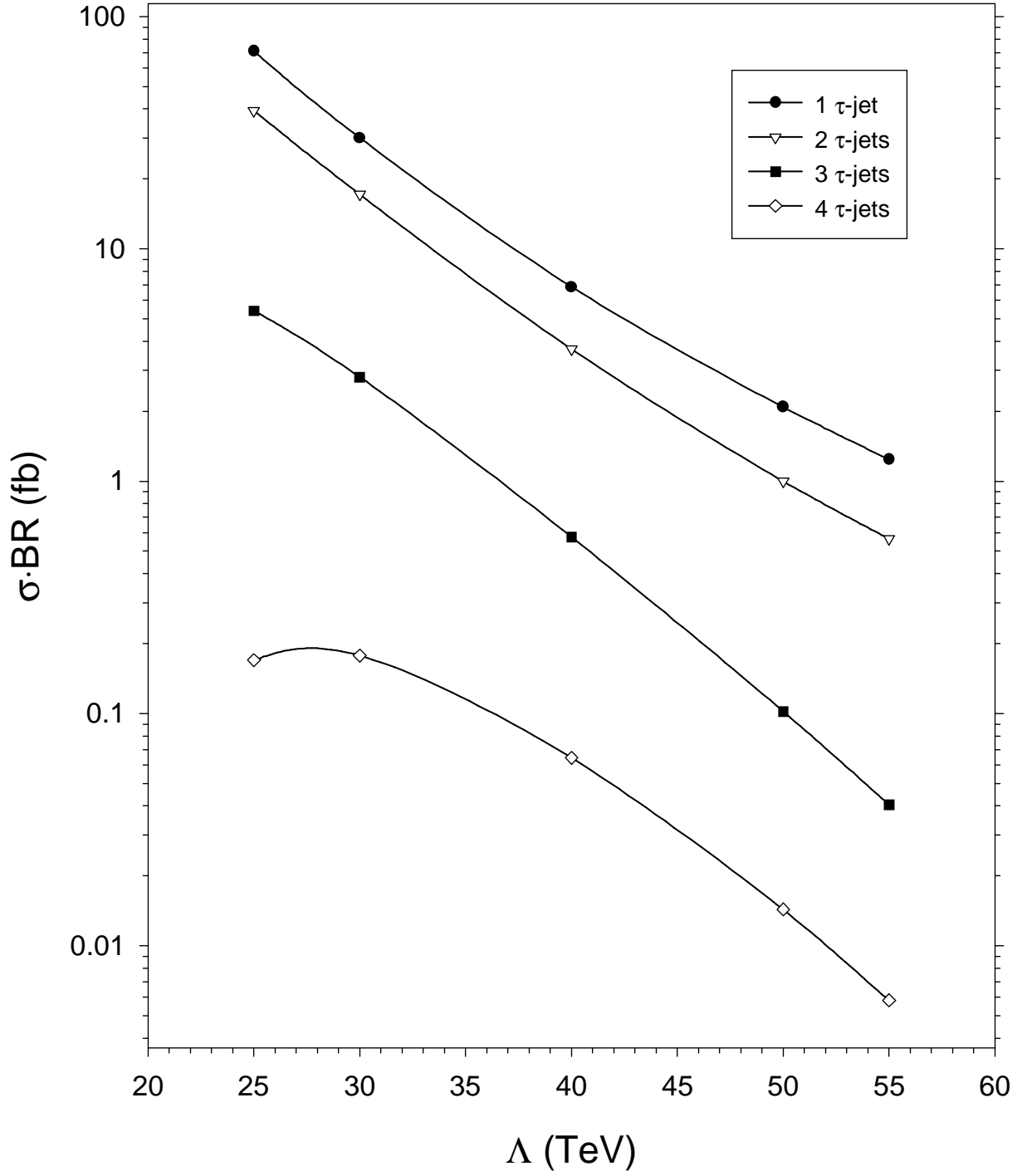


FIG. 14. $\sigma \cdot BR$ after cuts for the inclusive τ jets modes for the parameters $n = 3$, $\tan \beta = 15$ and $M/\Lambda = 20$.

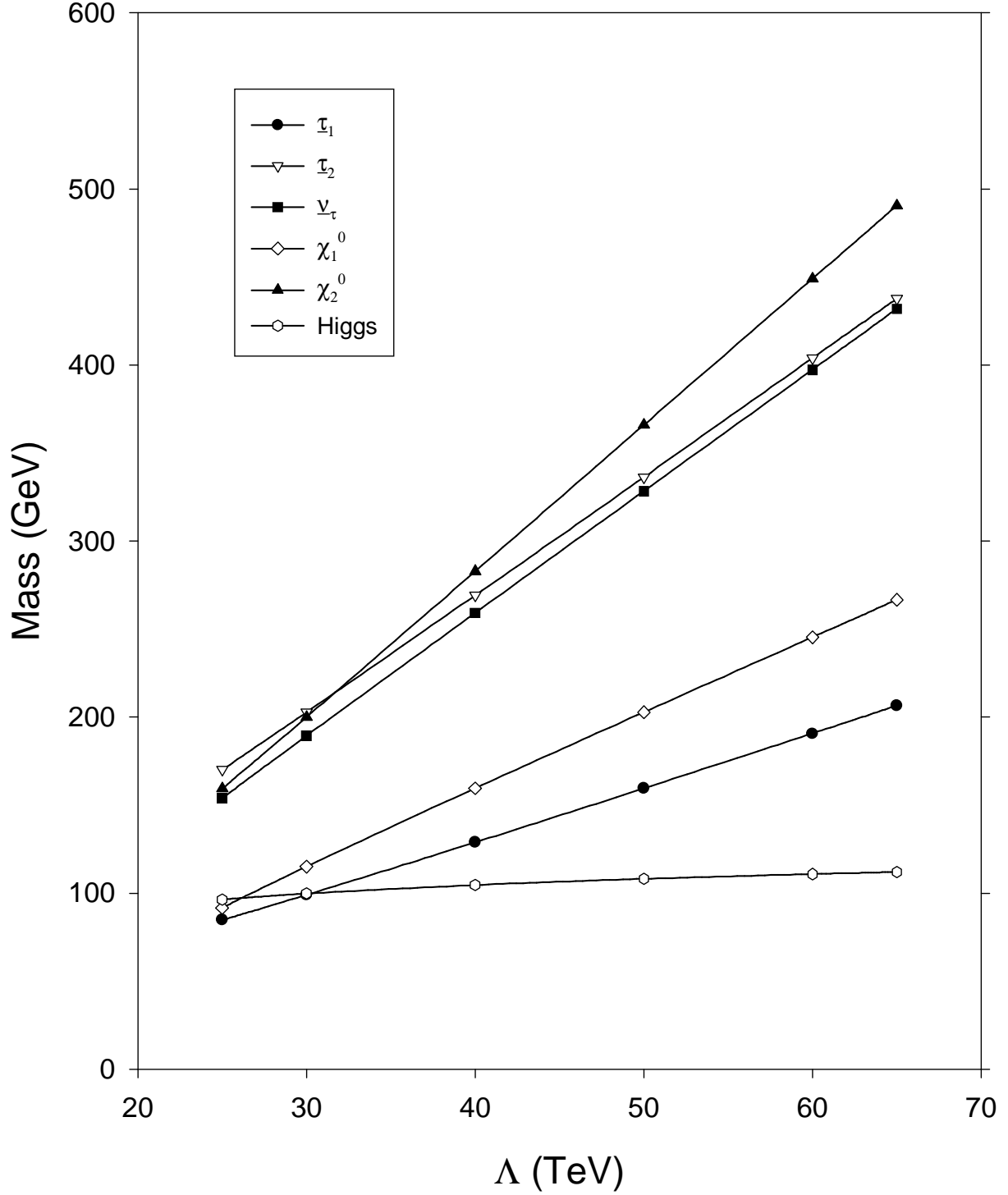


FIG. 15. The masses for the sparticles of interest for the co-NLSP example where $n = 3$, $\tan \beta = 3$ and $M/\Lambda = 3$.

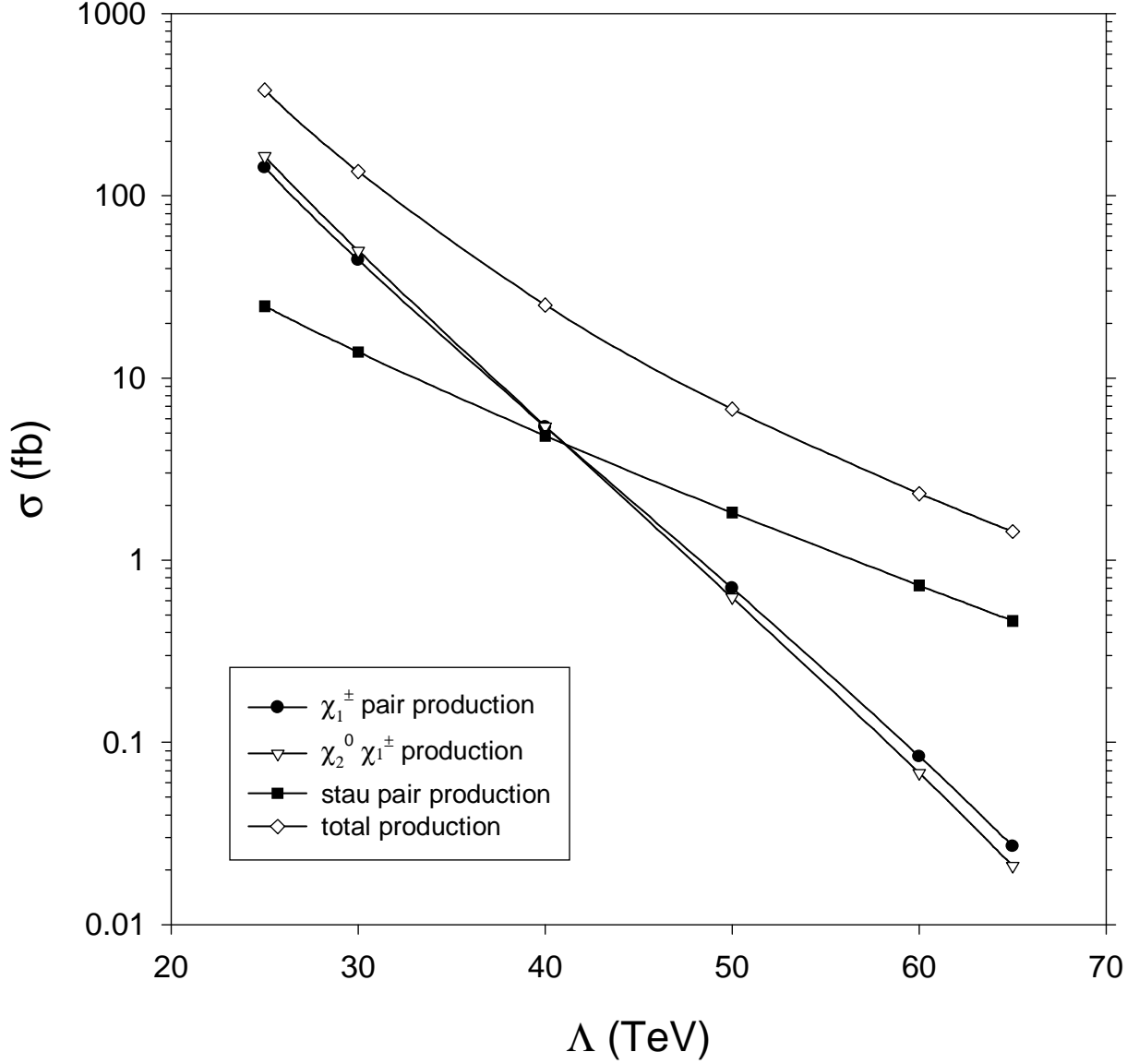


FIG. 16. The SUSY production cross sections for the co-NLSP example where $n = 3$, $\tan \beta = 3$ and $M/\Lambda = 3$.

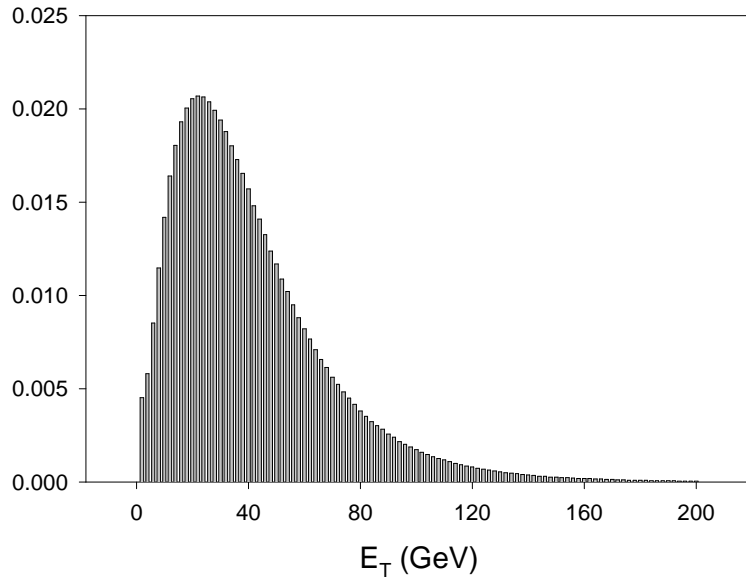
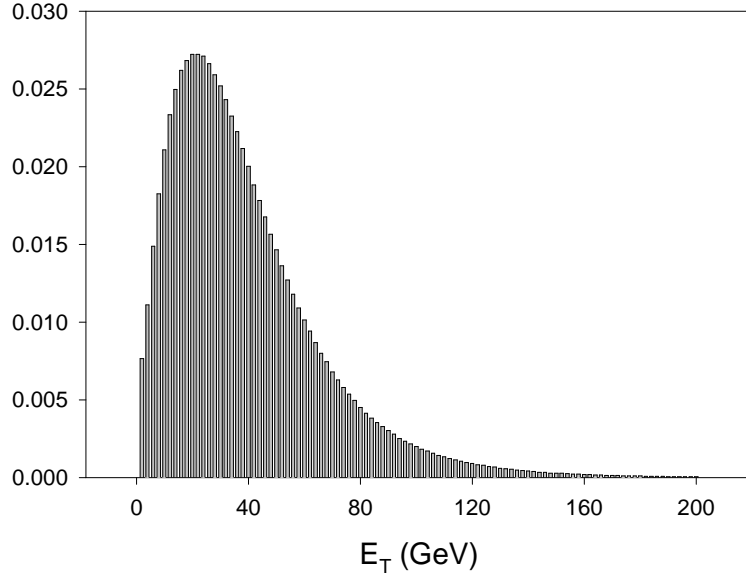
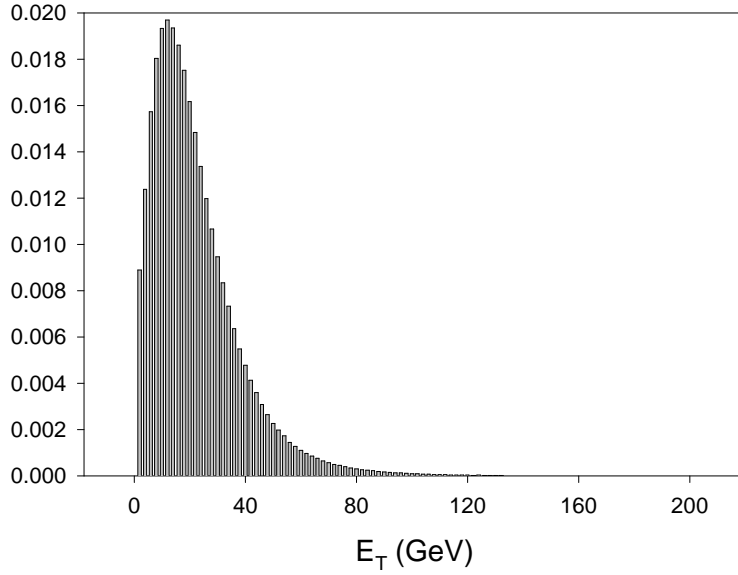
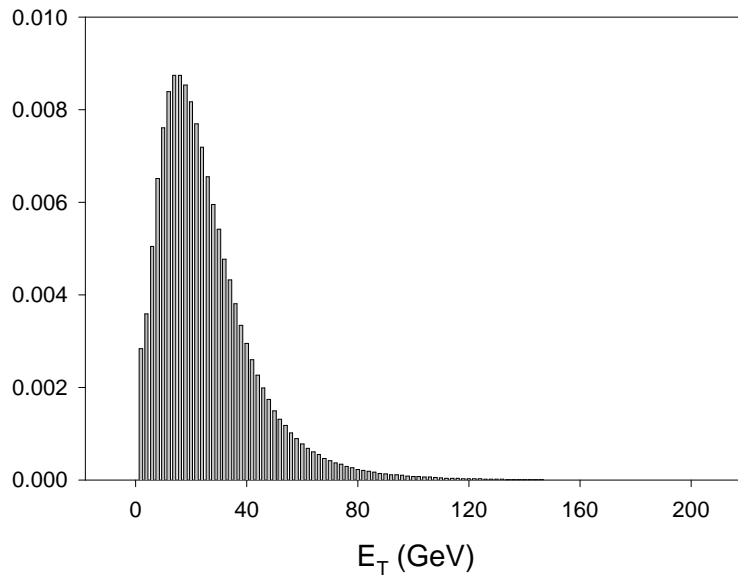


FIG. 17. The E_T distributions of the leading τ jet for the parameters $n = 3$, $\tan \beta = 3$, $M/\Lambda = 3$ and $\Lambda = 25$ TeV. In (a), no cuts have been imposed. In (b), the $|\eta| < 1$ cut on τ -jets has been imposed.

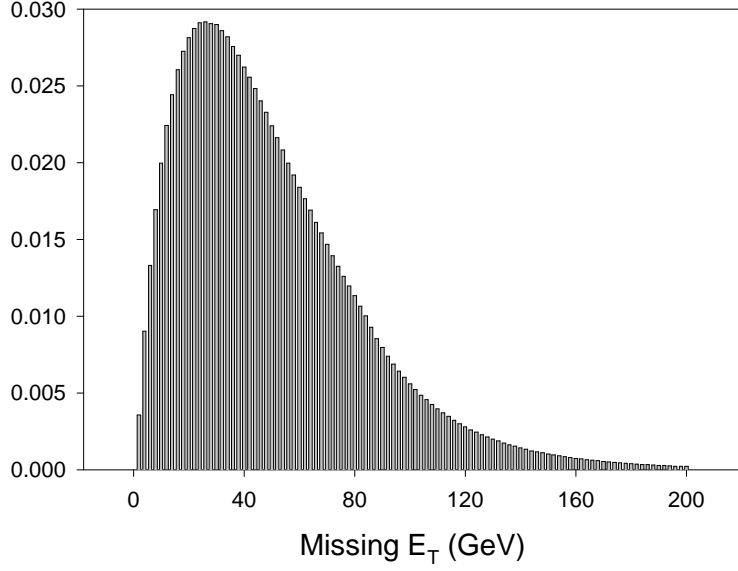


(a)

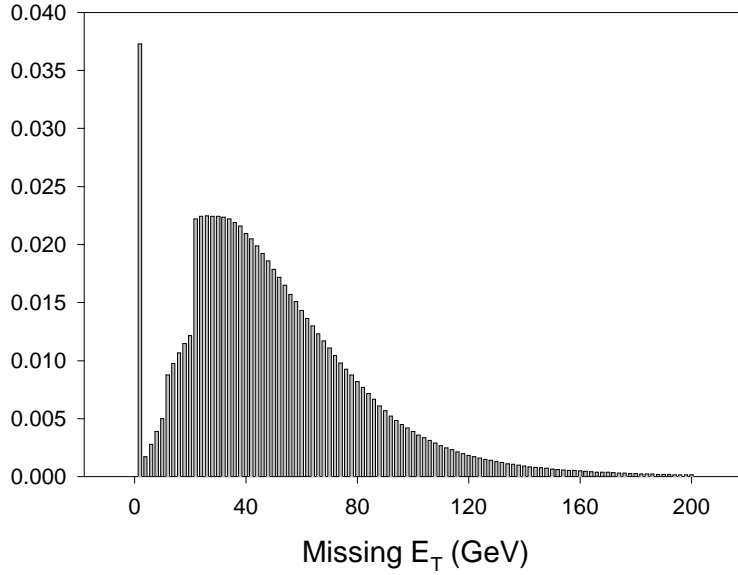


(b)

FIG. 18. The E_T distributions of the secondary τ jet for the parameters $n = 3$, $\tan \beta = 3$, $M/\Lambda = 3$ and $\Lambda = 25$ TeV. In (a), no cuts have been imposed. In (b), the $|\eta| < 1$ cut on τ -jets has been imposed.



(a)



(b)

FIG. 19. \cancel{E}_T distribution of the secondary τ jet for the parameters $n = 3$, $\tan \beta = 3$, $M/\Lambda = 3$ and $\Lambda = 25$ TeV. In (a), no cuts have been imposed. In (b), the E_T/p_T and pseudorapidity cuts on the jets and charged leptons have been imposed.

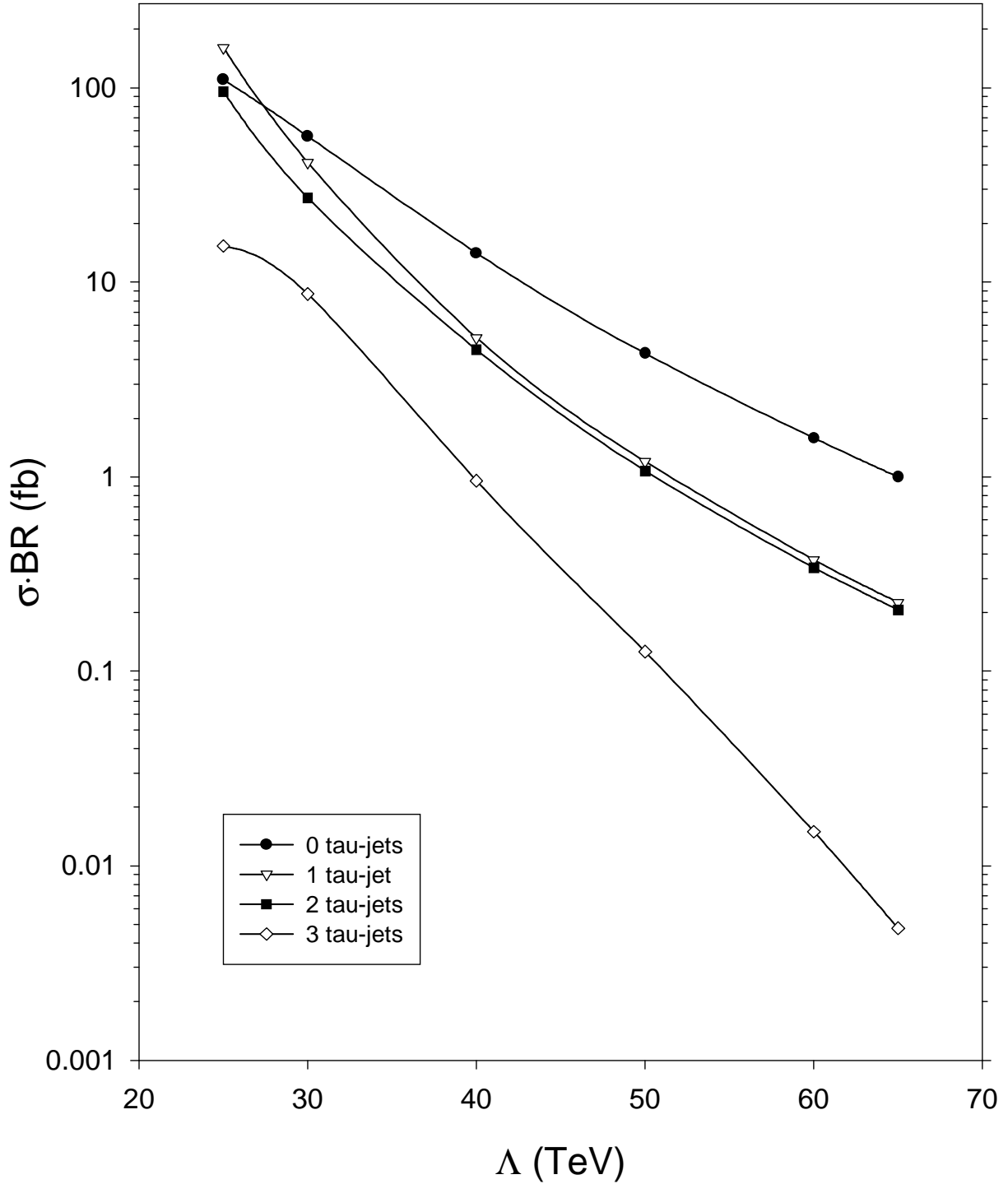


FIG. 20. $\sigma \cdot BR$ before cuts for the inclusive τ jets modes for the parameters $n = 3$, $\tan \beta = 3$ and $M/\Lambda = 3$.

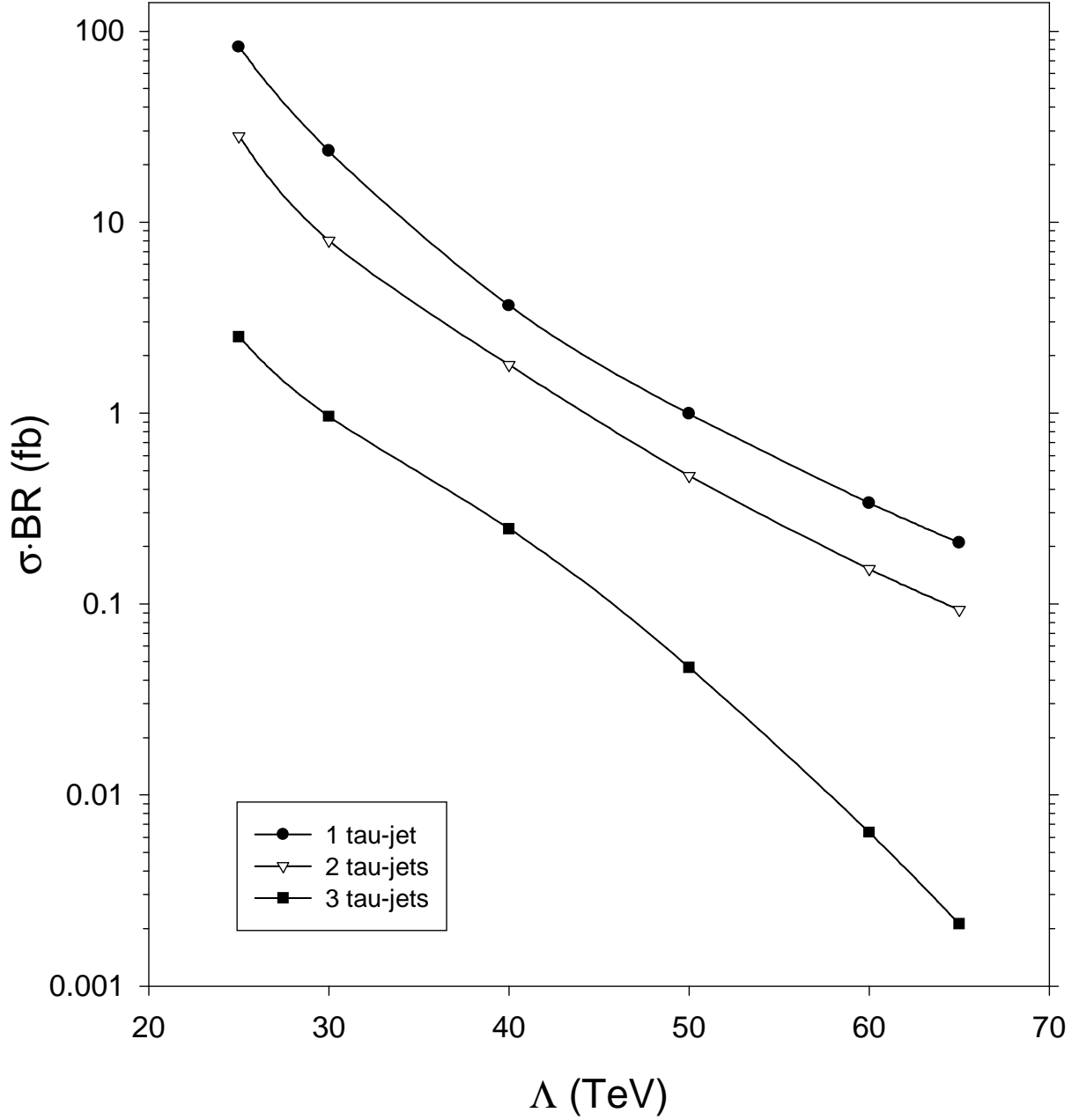


FIG. 21. $\sigma \cdot BR$ after cuts for the inclusive τ jets modes for the parameters $n = 3$, $\tan \beta = 3$ and $M/\Lambda = 3$.